KFKI-73-23
IAEA -855

F. Szlávik
G. Kosály
G. Kozman
D. Pallagi
P. Pellionisz

DEVELOPMENT OF CORRELATION INSTRUMENTS AND MEASUREMENT TECHNIQUES WITH SPECIAL REGARD TO THE APPLICATION OF CORRELATION METHODS IN NEUTRON PHYSICS AND REACTOR TECHNIQUES

(FINAL REPORT)

Hungarian Academy of Sciences

CENTRAL
RESEARCH
INSTITUTE FOR
PHYSICS

BUDAPEST

INTERNATIONAL ATOMIC ENERGY AGENCY
CONTRACT NUMBER: 855/R1/RB

FINAL REPORT

ON

"DEVELOPMENT OF CORRELATION INSTRUMENTS AND MEASUREMENT TECHNIQUES WITH SPECIAL REGARD TO THE APPLICATION OF CORRELATION METHODS IN NEUTRON PHYSICS AND REACTOR TECHNIQUES"

Chief Scientific Investigator:
FERENC SZLÁVIK

SEPTEMBER 1972

CENTRAL RESEARCH INSTITUTE FOR PHYSICS
BUDAPEST, HUNGARY

ABSTRACT

The Final Report considers the N° 855/R1/RB Research Contract work conducted at the Institute from 1970 to 1972. The work can be grouped in five main directions each dealt with in a separate section of this report. The fundamental background to the statistical investigations is covered by the two first sections, which discuss respectively developments in electronics and a special problem of the general theory of random processes. The third and fourth sections are devoted to two aspects of power reactor noise studies; firstly the theoretical treatment of special noise sources, and secondly, the experimental investigations on power reactor noise. The fifth section turns to a domain closely related to solid-state physics, that of correlation-type neutron spectroscopy.

РЕЗЮМЕ

В препринте обобщаются результаты исследований, проведенных в институте в 1970-1972 г.г. по контракту исследовательских работ № 855/R1/RB . Работа состоит из 5 глав, в каждой из которых рассматривается отдельная область исследований. В первых двух главах в общих чертах излагается основа стохастических исследований сигналов, т.е. говорится об усовершенствованиях, проведенных в области электронных приборов, а также об одной специальной проблеме общей теории случайных процессов. В 3-ей и 4-ой главах говорится о двух направлениях исследования шума энергетических реакторов: первое направление - теоретическое исследование специальных источников шума, второе - экспериментальное исследование шума энергетических реакторов. В пятой главе обсуждаются вопросы корреляционной нейтронной спектроскопии, тесно связанной с исследованиями в области физики твердого тела.

KIVONAT

A záró-report összegezi az intézetben 1970 és 1972 között folytatott, a 855/R1/RB kutatási szerződés alapján végzett kutatásokat. A munka öt fő területre osztható: a reportban mindegyikkel külön fejezet foglalkozik. Az első két fejezet a sztochasztikus jelvizsgálatok általános alapjait, nevezetesen az elektronikus készülékek terén végrehajtott fejlesztéseket, illetve a véletlen folyamatok általános elméletének egy speciális problémáját tárgyalja. A harmadik és negyedik fejezet teljestimény-reaktorok zajvizsgálatainak két aspektusával foglalkozik, amelyek közül az első speciális zajforrások elméleti, a második pedig teljesitmény-reaktorok zajának kisérleti vizsgálata. Az ötödik fejezet a korrelációs neutron-spektroszkópiát, a szilárdtestfizikai kutatásokhoz szorosan kapcsolódó területet tárgyalja.

CONTENTS

1. STATISTICAL INSTRUMENTATION TECHNIQUE

EDITED BY P. PELLIONISZ *

ABSTRACT

A short summary is given of the recent improvements in statistical instrumentation achieved at the Institute by researchers engaged in work under I.A.E.A. 855/R1/RB Research Contract.

The correlators used in the measurement of stochastic signals consist of a conventional multichannel analyzer combined with special plug-in units. Refinements of correlation technique as well as additional instrumentation /high-sensitivity ammeters, signal conditioner/ are also discussed.

1.1 Correlation instrumentation

1.1.1 Correlator KORALL-A

The initial step required in work at the Institute in the field of correlation measuring methods was the development of the basic correlation instrumentation. For measurements of stochastic signals we had a multichannel analyzer at our disposal, the NTA 512 Model developed and produced in the Institute. It was decided that the most effective way of developing the necessary special instrumentation was to use the multichannel analyzer as a basic instrument in combination with relatively simple, special plug-in units.

The first correlator, which was produced for measurements with pseudo-random chopping in the neutron spectroscopy /see 5.1/, was the KORALL-A equipment. This instrument is a specialized digital correlator [1.1],

* Acknowledgement

The editor is indebted to Messrs.F.Szlávik and G.Kozmann. Mr.F.Szlávik was co-author of developments in correlation instrumentation, while additional equipment was designed by Mr.G.Kozmann.

[1.2] for measuring the pulse-response function of linear systems with the aid of a pseudo-random modulation /Fig. 1.1/.

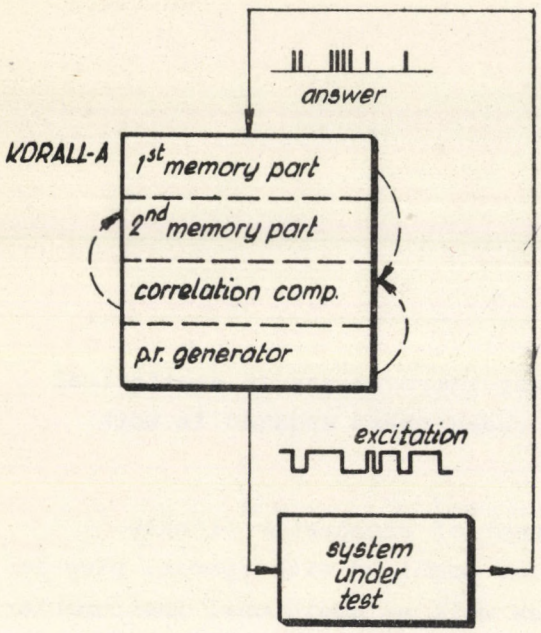

Fig. 1.1

Measurement of the pulse-response function of a system on the correlation principle using the KORALL-A digital correlator

The p.r. modulation sequence is generated by a built-in binary pseudo-random generator /n=8, N=255/. The periodic modulation produces a periodic response in the form of frequency-modulated pulse series at the output of the system to be investigated. This response is stored in the first half of the 512-channel ferrite core memory of the analyzer. Shift pulses from the pseudo-random generator also shift the address register of the memory, so that the time-channel width is equal to the time interval between subsequent pulses of the clock generator. When the number of counts in any channel attains a present value, the correlator stops the measurement and initiates the computing period. During this period the cross-correlation function of modulation and response /i.e. the pulse-response function of the tested system/ is calculated and stored in the form of 255 discrete ordinate values in the second half of the memory. Data from any sector of the memory can be displayed on a c.r.t. screen, punched or printed on paper tape, etc. During the computation period data in the first sector remain unchanged, so that any measurement can be continued making use of the previously accumulated data.

Detailed specifications of the equipment are given in Appendix 1.4.1.

1.1.2 Correlator KORALL-B

The second step in the instrumentation programme was the development of the general-purpose KORALL-B correlator [1.2]. This is a polarity correlator which permits the determination of auto- and cross-correlation functions of stochastic signals. It is again a combination of the NTA-512 analyzer and a special plug-in unit /Fig. 1.2/ operating on the following principle.

A clock signal generator causes the address register to overflow. The overflow signal drives the sampling /and polarity comparator/ units to send quantized /1-bit/ information about the instantaneous values of the input signals received from the two signal sources into the first element of the shift register and into the buffer register respectively. A new sampling always clears the first element of the shift register; the new information bit is written in its place and the whole content of the register is shifted by one step. Thus, the shift register always contains the last N bits of information from one of the measuring channels, in sequence of arrival.

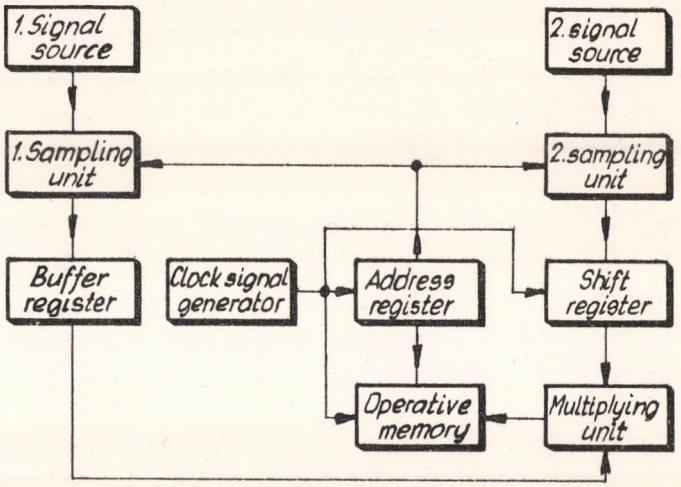

Fig. 1.2
Block diagram of the KORALL-B correlator

The products needed for computation of the correlation function are produced as follows. With the aid of the address register the clock generator successively reads the values stored in the shift register, and these bits are multiplied by the bits stored in the buffer register in the sequence they are read out. The product, the polarity bit, is sent by the address register and memory control circuits to the operative memory for addition on the bits already stored at the selected address.

It can be seen that in the channels of the ferrite core memory the points of the polarity correlation function for N shifts in time are generated in the corresponding channels of the memory simultaneously with the measurement. At the present stage of development the values are not normalized by the correlator.

If auxiliary signals are required /e.g. in the case of a non-Gaussian signal distribution/ built-in quasi-random generators are available. These generators are feedback circuits producing of negligible internal correlation.

The data stored in the equipment are displayed visually on the oscilloscope screen of the analyzer. Other output devices, such as printers, may also be connected to the analyzer.

Detailed specifications of the apparatus are given in Appendix 1.4.2.

1.1.3 Refinements in correlation instrumentation

In the course of the experimental investigations with the two correlators work was also devoted to the methodological problems of correlation measurements as well as with refinements in the construction of the correlators.

Among the methodological problems one of the most important is the dispersion of the short-term correlation functions. We examined how the error of the correlation function due to a finite measurement time is influenced by measuring time, sampling frequency, sampling size, etc. The error can be defined as

$$\sigma^2_{xy}(\tau;T) = \overline{\left[\phi_{xy}(\tau;T) - \phi_{xy}(\tau)\right]^2} \qquad /1.1/$$

where

$\sigma_{xy}(\tau;T)$ is the standard deviation of the correlation function measured for time T at a delay value of τ

$\phi_{xy}(\tau;T)$ is the correlation function measured for time T

$\phi_{xy}(\tau)$ is the correlation function measured for time $T=\infty$.

The value of σ^2_{xy} for the polarity correlator, in the case of Gaussian signals and infinite sampling rate, is given by

$$\sigma^2_{xy}(\tau;T) = \frac{2}{T}\int_0^T P_{xx}(\tau)\, P_{yy}(\tau)\, d\tau \quad , \qquad /1.2/$$

where

$P_{xx}(\tau)$ is the polarity auto-correlation function of the function x

$P_{yy}(\tau)$ is the polarity auto-correlation function of the function y.

The polarity correlation function P can be related to the general correlation function ϕ as

$$P_{xx} = \frac{2}{\pi} \arcsin \phi_{xx} \qquad /1.3/$$

$$P_{yy} = \frac{2}{\pi} \arcsin \phi_{yy} \qquad /1.4/$$

It can be seen that the standard deviation is $\frac{\pi}{2}$ times higher when using the polarity correlation method.

The auto-correlation function taken as a reference in the standard deviation measurements is shown in Fig. 1.3. Three sets of measurements were accomplished, each set representing an average obtained from 30 runs.

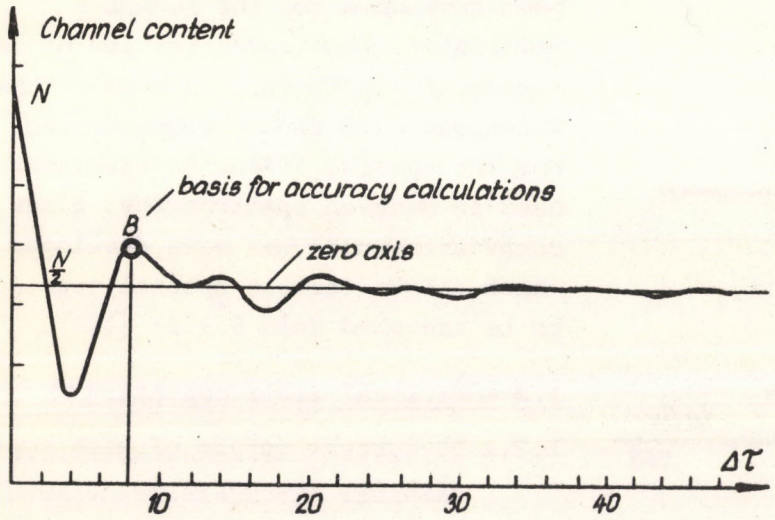

Fig. 1.3

$P_{xx}(\tau)$ experimental auto-correlation function of narrow-band noise

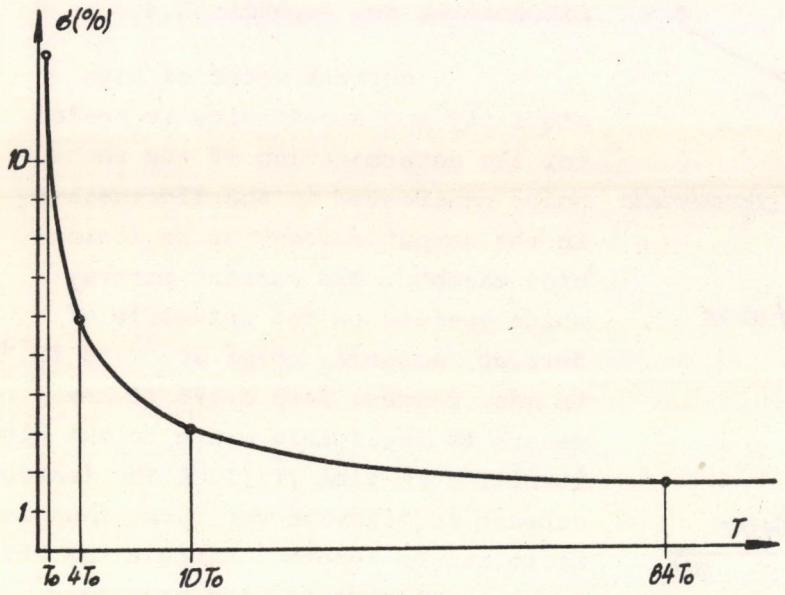

Fig. 1.4

Standard deviation of correlation measurements on narrow-band noise for f_M=const

The first set /Fig.1.4/ shows the influence of the measuring time on the standard deviation error. Here the sampling frequency was kept at a constant value. The measured curve confirms the theoretical expectations: it obeys a quadratic rule.

The second set of measurements /Fig. 1.5/ follows the error of the auto-correlation function P_{xx} versus sampling frequency. Here the measuring time was kept at a constant value. It can be seen from the curve that above the Nyquist frequency the measuring accuracy cannot be inproved further. Below this point, increasing sampling frequency leads to higher accuracy, because sampling size is also increased.

The third set of measurements /Fig. 1.6/ gives the error of the auto-correlation function P_{xx} versus sampling frequency, for constant sampling size /number of samples/. It can be seen that at the unnecessary high sampling frequencies the accuracy

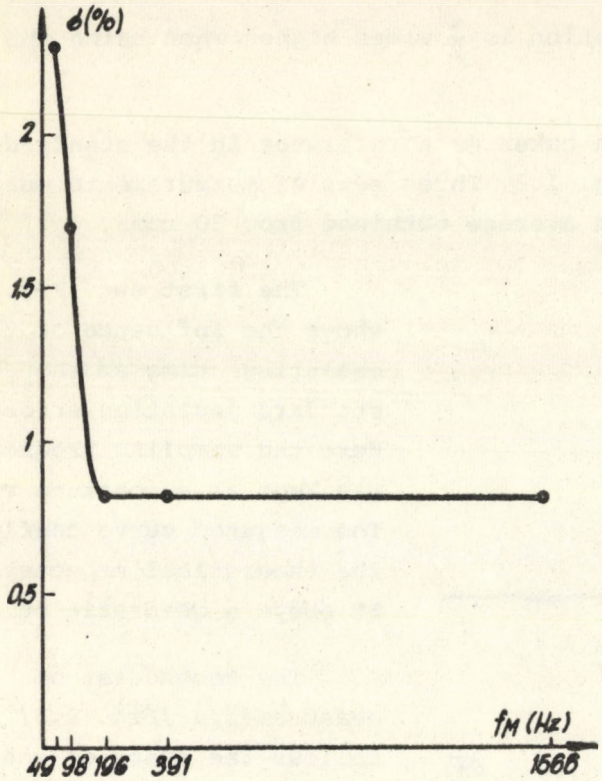

Fig. 1.5

Standard deviation of correlation measurements on a narrow-band noise for T_{meas}=const

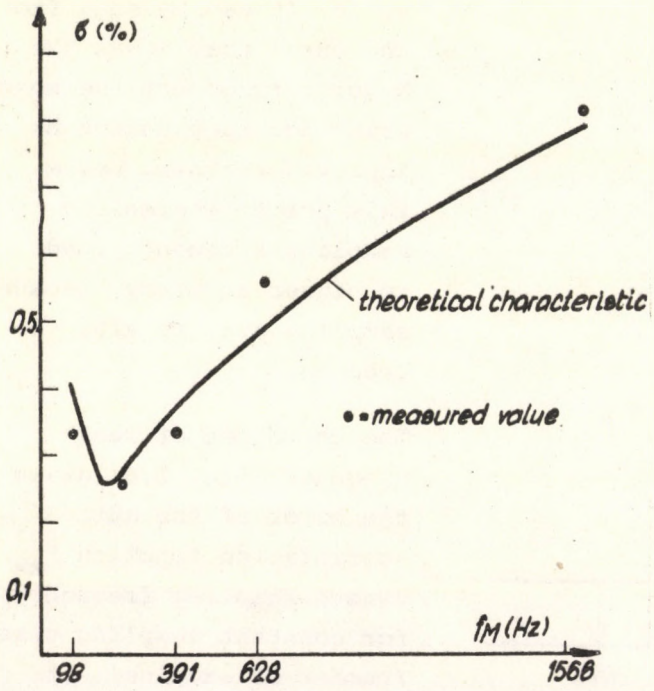

Fig. 1.6

Standard deviation of correlation measurements on a narrow-band noise for N=const

of the measurements improves with decreasing sampling frequency. Below the Nyquist-frequency, however, this effect is offset by a loss of information.

As for the technical refinements, a modified input circuitry has been developed for the KORALL-B correlator after investigation of zero instability effects, and some of the functions have been perfected, etc. For the special KORALL-A correlator used in neutron spectroscopy, a new computation unit has been developed which allows certain special functions to be executed /see 5.3.2/ [1.3].

1.2 Additional instrumentation

1.2.1 DC current meters of high sensitivity for noise measurements

A necessary and important part of activities was devoted to the development of the NV-252 Picoammeter and NV-253 Femtoammeter units [1.4]. For detailed specifications of the Picoammeter see Appendix 1.4.3.

A current meter of high stability and sensitivity is needed for the determination of the reactor noise manifested in the fluctuation in the output current of an ionization chamber. The current meters, which operate on the principle of current feedback, cover 10^{-15} to 10^{-3}A in many ranges. Zero drift of the meters is negligible owing to the high stability in time /1%/12^{h}/. The leakage current is likewise very low, thus its noise can be ignored. Since a MOS FET input transistor is used, the low-frequency fluctuation of the offset voltage can be appreciable because of the 1/f relation. The contributions

from offset voltage noise to the output noise grows with increasing input capacitance. The transfer function for the offset noise is expressed by

$$\frac{U_{out}(p)}{U_{noise}(p)} = \frac{A(p)}{1 + A(p)\,\frac{Z_g(p)}{Z_g(p) + Z_f(p)}} \qquad /1.5/$$

where p is the Laplacian operator, and $A(p)$, $Z_g(p)$ and $Z_f(p)$ stand for the Laplacians of the gain, input impedance and feedback impedance, respectively. The input impedance of the detector and the cable is primarily capacitive, while the feedback impedance is a parallel RC network. Substituting

$$Z_g = \frac{1}{pC_g} \qquad /1.6/$$

and

$$Z_f = \frac{1}{1 + pR_f C_f} \qquad /1.7/$$

into /1.5/, it can be seen that even at relatively low frequencies C_g causes a considerable rise in the output noise level.

The importance of the input impedance is illustrated in Fig.1.7, which gives the amplification factors of the input offset voltage noise in different ranges. In technological reactor noise measurements the frequency band of 0-10 Hz is of primary interest.

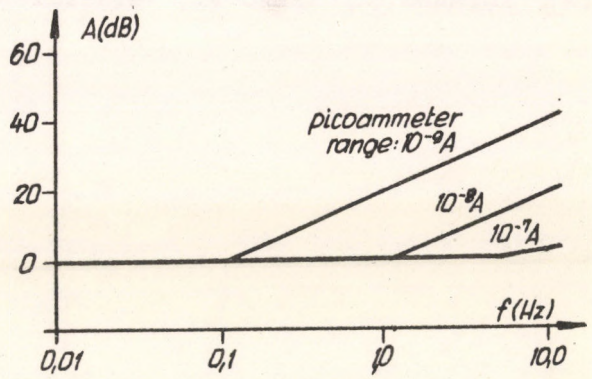

Fig. 1.7
Amplification of the offset voltage noise components

1.2.2 Four-channel signal conditioner

The measurement of stochastic signals puts great importance on the conventional measuring electronics placed between the data source /e.g. a noisy system/ and the data-processing equipment /e.g. a correlator/. If the frequency spectrum of the signal to be analyzed has components of higher frequency than that allowed by the maximum sampling frequency of the correlator, low-pass filters must be used. Generally, the output signal of the data source must be amplified or attenuated, and in many cases the base-line level must be modified also.

In order to facilitate this sort of data-handling, a four-channel signal conditioner has recently been developed. Each channel has a DC-amplifier with variable gain, a low-pass filter of variable bandwidth, and base-line shift possibility. This device greatly expedites use of the Telefunken MAS 54 four-channel magnetic tape recorder, delivered by the I.A.E.A. for noise measurements.

Some of the most important parameters of the equipment are:

Gain	: 10; 20; 50; 100; 200; 500; 1000;
Upper frequency limit	: 10; 20; 50; 100; 200; 500; 1000; 2000 Hz
Base-line shift	: +10 V ..... -10 V
Input noise max.	: 20 μV_{eff}
Stability	: 4 $\mu V/^{o}C$; 4 μV/10 hours

1.3 References

[1.1] PÁL,L., KROÓ,N., PELLIONISZ,P., SZLÁVIK,F., VIZI,I. Symp. on Neutron Inelastic Scattering, Copenhagen, 1968. Vol. 2, p. 407.

[1.2] PELLIONISZ,P., SZLÁVIK,F. Mérés és Automatika, IV /1967/ 7-8.

[1.3] PELLIONISZ,P., KROÓ,N. Symp. on Neutron Inelastic Scattering, Grenoble, 1972. I.A.E.A./SM-155/F-8.

[1.4] KOZMANN,G., IMEKO V., Versailles, 1970.

APPENDIX 1.4.1

MAIN SPECIFICATIONS OF THE KORALL-A CORRELATOR

The apparatus consists of

a KFKI NTA-512 MULTICHANNEL ANALYZER, and
a KFKI NE-283 CORRELATOR plug-in unit.

System features
- built-in binary pseudo-random generator /255 steps/
- correlogram between input and output signals of the system to be tested /255 channels/
- ferrite core memory /512x16 bits/

Modes of operation
- Measurement: registration of the system's response
- Data processing: correlogram evaluation

Time channels
- number of channels: 2x255
- channel width: $n \cdot 10^m$ μsec
  for n = 2; 5; and m = 1; 2; 3; 4; 5; 6; 7; 8.
- same channel width for response recording and correlogram

Preset facilities for channel contents in Measurement mode
2^8; 2^{10}; 2^{12} pulses

Input data
- pulses of -6 V amplitude accepted
- maximum counting frequency: 1 MHz

Correlogram evaluation
- follows Measurement mode, either manual or automatic start
- computation time: max. 2 sec.

APPENDIX 1.4.2

MAIN SPECIFICATIONS OF THE KORALL-B CORRELATOR

The apparatus consists of

a KFKI NTA-512 MULTICHANNEL ANALYZER, and
a KFKI NE-299 CORRELATOR plug-in unit.

System features
- real time
- polarity correlation
- ferrite core memory

Modes of operation
- Auto - XX
- Cross - XY
- Auto - YY
- AC or DC in each mode

Delay

Number of elementary delay intervals /n/	32	64	128	256	512	1024
Min.duration of the elementary delay interval /$\Delta\tau$/ [msec]	0.64	1.28	2.56	5.12	10.24	20.48
Min. total delay /$n \cdot \Delta\tau$/ [msec]	21	84	330	1310	5250	21000
Oscilloscope sensitivity for delay time [msec/cm]	33	33	33	131	525	2100

Memory

Capacity : 2^{15}/channel
Limit of the channel content displayed on the internal oscilloscope : 2^8, 2^{10}, 2^{12}, 2^{14}, 2^{16}
Preset facilities for the channel contents : 2^8, 2^{10}, 2^{12}, 2^{14}, 2^{16}

Display and read-out of channel contents

built-in cathode-ray tube
numerical indicator tubes
perforator
printer
X-Y plotter

Input data /for X and Y channels/

Input impedance	: 25 kOhm
Input signal	: 0.4 V p-p...40 V p-p
Internal compensation voltage in DC operation	: max. $\pm$ 12 V
Input D.C. voltage in AC operation	: max. 150 V
Frequency-band in DC operation	: 0 - 1 kc/s
Frequency-band in AC operation	: 0.1 c/s - 1 kc/s

Auxiliary signals /for H_x and H_y channels/

EXT; H_1; H_2
may be added to input signals.

EXT - any external signal of max. 10 V p-p

H_1 - from a built-in pseudo-random generator producting 31 equidistant /320 mV/ voltage levels with a total sequence-length of 1023

H_2 - from a built-in pseudo-random generator /statistically independent of H_1/ producing 31 equidistant /320 mV/ voltage levels with a total sequence-length of 2047.

APPENDIX 1.4.3

SPECIFICATIONS OF THE NV-252 LIN-LOG PICOAMMETER

Linear Channel:

Current ranges	: 10^{-3} A to 10^{-12} A in decadic ranges
Zero stability	: max. 1%/8 hours
Temperature stability	: max. 0.4%/^{o}C
Current polarity	: positive or negative
Accuracy	: ± 2% /10^{-3} A to 10^{-10} A/
	± 2.5% /10^{-11} A/
	± 5% /10^{-12} A/
Offset current	: max. 10^{-13} A

Logarithmic Channel:

Current polarity	: positive
Input current	: 10^{-10} A to 10^{-3} A /in one range/
Zero stability	: 0.02 decade/^{o}C

General:

Power	: 220 V; 50-60 Hz
Weight	: 9 kg
Operating temperature range	: + 10^{o}C .....+ 40^{o}C.

2. NON-PARAMETRICAL DETECTION METHODS

EDITED BY G. KOZMANN AND F.SZLÁVIK

ABSTRACT

Some fundamental problems in the monitoring of noisy systems that were tackled within the scope of I.A.E.A. Research Contract No. 855/R1/RB are discussed. A review is presented of the Kolmogorov-Smirnov method, which has proved an effective tool for the fast detection of certain changes in stochastic processes. The consistency of Kolmogorov-Smirnov decisions is considered in detail.

For technical implementation of the method the effect of the quantization error also needs to be taken into account. An approach to this problem is described and information is given on the construction and functioning of a Kolmogorov-Smirnov detector based on a TPA small computer.

2.1 Introduction

In work with potentially dangerous and/or costly systems reliable and safe operation is obviously a prime objective. On the other hand, the monitoring of the momentary state of such systems is becoming an increasingly complicated task as a result of the continual sophistication they undergo and the growing number of parameters and intervention possibilities which this sophistication usually entails. Moreover, some parameters are not, in fact, directly measurable, while the measurement of others may require such laborious data evaluation as to exceed available computing facilities. At times, therefore, the amount of data-handling imposed by advances in instrumentation can be bewildering, and particularly so if the need is for speedy information in a form that is readily assimilated by a system operator. From this point of view "noise monitoring" is becoming increasingly important as a data-condensing strategy, because the noise of a system reflects, with greater or lesser weighting, the effects of all the system parameters. Thus the importance of the statistical properties

of a noise spectrum is that they can not only furnish concise information about the measurable parameters of the system, but they can also reveal the influence of factors which are either unmeasurable or, at present, not directly measurable.
A well-founded, concise "situation report" which can keep the operator currently aware of the state of the system makes it possible to utilize the computer which controls the system also for other tasks in time-sharing operation.

Within the framework of I.A.E.A. Research Contract No. 855/R1/RB methods have been introduced and/or refined for analysing noises in the low-frequency /max. 1 kHz/ region, a range which seems to cover a number of problematical cases. More specifically, this work has been concerned with analysis of the pulse-height distribution of low-frequency noise and calculation of the correlation function or power density function. In part this has involved an investigation of means for detecting imminent changes in the states of noisy systems. The outcome has been that we are now in a position where we are able - provided a close correlation can be assumed to exist between the noise and the technical and physical parameters of a system - to diagnose when the state of the system is approximately that of a reference state. The crucial point here is obviously the assumption of a close correlation between the noise and the factors which influence the system, as acceptance of the technique clearly stands or falls on the question of whether this assumption is justified in practice by statistical measurements and theoretical calculations.

For diagnosis from pulse-height distributions the Kolmogorov-Smirnov method is applied. This section goes over the arguments prompting this choice as well as the principles of the method, and finally it discusses the chief problems met in its implementation, some of which were not considered in the earlier Progress Reports.

2.2 Fundamental problems of system diagnostics, arguments for choice of method

2.2.1 Efficiency

Observations that are costly in terms of time and money, as is frequently the case with biological, economic and also reactor diagnostic problems, need to be collected in a manner that permits optimum use of a minimum of data in the final analysis. Experimental arrangements should consequently be designed to enable one to use the most appropriate analytical methods.

As major calculational problems may sometimes arise in the evaluation of results one is naturally led to consider the possibilities offered by the advent of computers.

2.2.2 Non-parametric detector vs "optimum detector".

In most treatments of detection theory special emphasis is laid on the concept of the optimum detector which calls for an essentially complete statistical description of the input signals and noises. However, there may be reasons why other, non-optimum detectors ought also to be considered, e.g.

/i/ when a complete statistical description of the input phenomenon is not available at the time the detector must be developed;

/ii/ if the statistics of the input data set vary with time or from one application to another; or

/iii/ if the optimum detector is too complex for practical implementation.

It is hardly surprising, then, if in the statistical literature special attention has been paid to developing methods of compensating for non-optimality with a "distribution-free" character; that is, with methods whose validity is independent of the distribution of the variables.

It can be shown that distribution free criteria can be obtained only in terms of the ordering relations between the sample elements [2.1]. This is the principle of the Kolmogorov-Smirnov detection method.

During the search for optimum properties or in the pursuit of general validity it must be kept in mind that the correctness or error of our conclusions concerning the reference populations depend exclusively upon the situation that exists in the sample, and not on the true "state of affairs" in the reference population /in the observed system/.

2.2.3 Goodness of fit, consistency

Among the possible methods of statistical examination tests of goodness of fit are the most suitable for system diagnostic purposes. In these tests one has to decide whether a collection of n independent samples has or has not been taken from a set characterized by a given, often only empirically obtained, reference distribution function. It is obvious that

errors can be made in this type of examination but it is imperative that with an increasing number n of samples the error probability should tend to zero; that is, the chosen method of examination must be consistent.

2.3 Basic properties of the Kolmogorov-Smirnov tests

Among the many distribution-free tests available for use in signal detection is a group of non-parametric statistics generally called the Kolmogorov-Smirnov tests. As statistics, these tests make use of various functional forms of the difference between two empirical distribution functions or between an empirical and an "exact" distribution function.

Consider the problem of deciding whether two sets of samples, of size n_1 and n_2, respectively, derive from the same underlying distribution. Let $X_2 = \xi_1, \xi_2 \cdots \xi_{n_1}$ and $X_2 = \eta_1, \eta_2 \cdots \eta_{n_2}$ be vectors representing the samples from populations F and G. The empirical distribution function for the samples X_1 and X_2 by $F_{n_1}(x)$ and $G_{n_2}(x)$ can be defined as

$$F_{n_1}(x) = \frac{1}{n_1} \sum_{i=1}^{n_1} u(x - \xi_i) \qquad /2.1/$$

$$G_{n_2}(x) = \frac{1}{n_2} \sum_{i=1}^{n_2} u(x - \eta_i) \qquad /2.2/$$

where $u(x)$ is the unit step function

A measure of the validity of the hypothesis, that vector samples X_1 and X_2 originate from the same underlying distribution, is some function of the difference between the empirical distribution functions $F_{n_1}(x)$ and $G_{n_2}(x)$, which we can call the distance function D, represented by the expression

$$D = \mathcal{F}\left\{F_{n_1}(x) - G_{n_2}(x)\right\}$$

where $\mathcal{F}$ represents some functional over the range of the variable x. The choice of the functional $\mathcal{F}$ is determined by the particular application.

Several forms of the functional $\mathcal{F}$ have been analyzed for their distribution under the zero hypothesis, in particular the point forms of the statistic

$$D_+ = \sup_{-\infty<x<\infty} \left\{ F_{n_1}(x) - G_{n_2}(x) \right\} \qquad /2.3/$$

$$D = \sup_{-\infty<x<\infty} \left| F_{n_1}(x) - G_{n_2}(x) \right| \qquad /2.4/$$

For the comparison of empirical distribution functions, Smirnov has proved the following two theorems for the case $n_1 = n_2 = n$:
Theorem 1: If $F(x) \equiv G(x)$, then

$$\lim_{n\to\infty} P\left(\sqrt{\frac{n}{2}} \sup_{-\infty<x<\infty} \left[F_n(x) - G_n(x) \right] < y \right) = \begin{cases} 1 - e^{-2y^2} & , \text{ if } y>0 \\ 0 & , \text{ otherwise} \end{cases} \qquad /2.5/$$

Theorem 2: If $F(x) \equiv G(x)$, then

$$\lim_{n\to\infty} P\left(\sqrt{\frac{n}{2}} \sup_{-\infty<x<\infty} \left| F_n(x) - G_n(x) \right| < y \right) = \begin{cases} K(y) & , \text{ if } y>0 \\ 0 & , \text{ otherwise} \end{cases} \qquad /2.6/$$

Here $$K(y) = \sum_{k=-\infty}^{\infty} (-1)^k e^{-2k^2y^2}$$

For the comparison of empirical and exact distribution functions the theorems which hold for two different distances between the points are as follows. Theorem 3 /Smirnov/:

$$\lim_{n\to\infty} P\left(\sqrt{n} \sup_{-\infty<x<\infty} \left[F_n(x) - F(x) \right] < y \right) = \begin{cases} 1 - e^{-2y^2} & , \text{ if } y>0 \\ 0 & , \text{ otherwise} \end{cases} \qquad /2.7/$$

Theorem 4 /Kolmogorov/:

$$\lim_{n\to\infty} P\left(\sqrt{n} \sup_{-\infty<x<\infty} \left| F_n(x) - F(x) \right| < y \right) = \begin{cases} K(y) & , \text{ if } y>0 \\ 0 & , \text{ otherwise} \end{cases} \qquad /2.8/$$

Another form of the Kolmogorov-Smirnov test is obtained through integration of the range of the variable rather than by using a point determination. The distance function considered is the weighted mean square difference in empirical distribution functions. /This is the method proposed by Cramer and von Mises [2.2]./

The decision function R of a detector designed in accordance with equations [2.5], [2.6], [2.7] and [2.8] can be expressed as

$$R = \begin{cases} 0, & \text{if} \quad y = D < D_\alpha \\ 1, & \text{if} \quad y = D \geq D_\alpha \end{cases} \qquad /2.9/$$

where $R = 0$ implies the basic $R = 1$ the alternative hypothesis. The latter decision means, of course that there is a significant change in the distribution function of the system noise./

In the choice of the decision limit D_α several further considerations need to be made. Errors in testing compliance with a statistical hypothesis /say,H_o/ may be of two types:

/i/ the hypothesis is wrongly rejected when it is true /false alarm/

/ii/ the hypotesis is wrongly accepted when it is false /false dismissal/

We may refer to these as errors of Type I and Type II, respectively. The probability of a Type I error is usually symbolized by α; the probability of a Type II error is, of course, a function of the alternative hypothesis /say H_1/ and is usually symbolized by β. The complementary probability $1 - \beta$ known as the power of the test of the hypothesis H_o against the alternative hypothesis H_1. /The specification of H_1 is obviously essential./

It follows immediately from the above that the acceptance or rejection of the original hypothesis depends very critically on the alternatives against which it is tested. In the Kolmogorov-Smirnov method based on the two different types of distances between points, the values of α are

$$\alpha_+ = e^{-2D_+^2} \qquad \text{and}$$

$$\alpha = 1 - K(D) \quad ,$$

if D_+ and D are the values of the distance y associated with the corresponding decision limit.

Let us see how α is determined in the case of system monitoring. It is natural to suggest in the first place that α should be chosen to be as small as possible in line with some acceptable criterion. However, even when testing a simple H_o against a simple H_1 only two of the quantities n, α and β can be fixed. If n is fixed, the Type I error probability α can generally be lowered only at the expense of raising the Type II error probability β. If, on the other hand, the sample size is a matter of free choice, it can in most cases be ensured that n will be

large enough to reduce both α and β to a reasonable level - though there is no "optimum" combination of α, β and n applicable to any given problem.

In this connection, one of the essential requirements which has to be met by any test of a statistical hypothesis is the consistency of the method used /see 2.2.3/. We have found while studying the theory of Kolmogorov-Smirnov detectors that for a detector designed around a given α according to the criterion $D > D_\alpha$ of [2.9] this consistency depends on H_1. In practice the detector may be inconsistent in a particularly large percentage of cases if α is chosen too low.

A Kolmogorov-Smirnov detector working consistently in every case can be designed only after examining, by repeated measurements, the convergence on the entire D distribution function and not that on a single arbitrarily chosen D_α level. This can be easily verified on inspection of the typical example depicted in Fig. 2.1, which shows how the D_{max} distribution corresponding to the assumption H_o deviates from that corresponding to assumption H_1 characterized by $F_1/x/ = F_o/x-x_o/$.

In the case presented, the limit $D_1(\alpha_1)$ is obviously less favourable than $D_2(\alpha_2)$ - even though $\alpha_1 < \alpha_2$ - since with the former the effect of H_1 is much less pronounced even if x_o is very large.

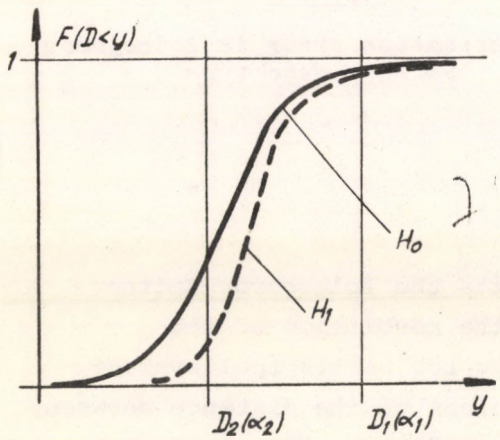

Fig. 2.1

Effect of the value of the decision limit on the probability distribution function with argument D < y for a simple shift in the variable x.

2.4 Effects of the quantization error

One problem of immediate practical importance arises from the fact that the construction of a set of "ordered" samples or "empirical distributions" corresponding to the original Kolmogorov-Smirnov equations assumes a quite precise knowledge of the probability variables. If in

practice this condition cannot be met /which is often the case with digital machines/, the relationships will hold in a form departing from theoretical expectation.

The error attributable to quantization is illustrated in Fig. 2.2. If the quantization step Δ is fairly large, more than one sample element may fall into some or all intervals of length Δ. If this is so, it may happen that the actual distance between the functions F and G in a given interval will be longer than the distance measured at the bounds of the interval. /Of course, it is supposed that samples are rounded down or up for each Δ interval./ This will evidently lead to a wrong decision if this has to be taken exactly at the point that apparently "reduces" the maximum distance between the functions.

---- rounded up
-.-. rounded down
/Both D_{up} and D_{down} are smaller than D^*/

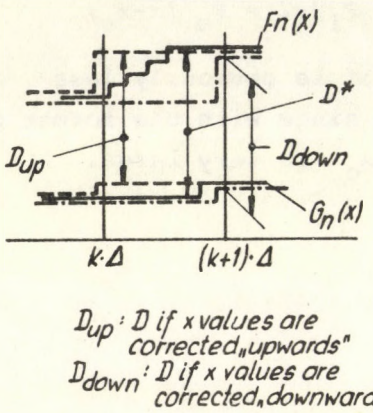

Fig. 2.2

The quantization error in Kolmogorov-Smirnov detection

A formula has been derived which permits the Kolmogorov-Smirnov equations to be generalized to the case where the resolution of the quantization is limited. /We have shown that, on the statistical average, correct results are obtained if the detected values of the distance between $F_n(x)$ and $G_n(x)$ are multiplied by a correction factor $\frac{2n}{m}$, where $m = m(F(x),\Delta)$, which can be estimated most simply from trial measurements./

The results have been verified by measurements on random signals from a Brüel and Kjaer white noise generator with a set-up consisting of a Kolmogorov-Smirnov detector based on a TPA-1001 small computer and a program elaborated specially for this particular type of evaluation [2.4].

The effect of the quantization error can be summarized from the

above considerations as follows. The ideal Kolmogorov-Smirnov detector is non-parametric; that is, it yields results in the form of significances independent of the distribution F(x) which characterizes the null hypothesis. On the other hand, detectors with quantization errors are not non-parametric. In the latter cases the actual value of α is sensitive to the nature of the measured distributions /though this dependence can be minimized by choosing n to be not too high and by utilizing high resolution A/D converters/. In order to reduce this negative effect it is advisable to set the gain of the data amplifier of the measuring set-up /see Fig. 2.3/ so that the input signals to the A/D converter cover as much as possible of the amplification range, while setting the variable resolution to the maximum value.

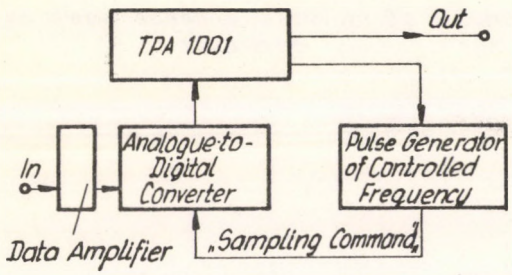

Fig. 2.3
Lay-out of a Kolmogorov-Smirnov detector

2.5 Independence of sample elements

Special attention has to be paid to the choice of the sampling frequency, because the Kolmogorov-Smirnov equation only hold if the sample elements are statistically independent.

In the case of a band-limited white noise the sampling frequency theoretically sufficient to ensure statistical independence of the sampled elements can be evaluated from a simple formula, for here non-correlation, and hence independence, can be guaranteed by adhering to the sampling prescription of SHANNON. In other cases the sampling frequency has to be reduced below the SHANNON frequency.

In our system the detector schedule was worked out so that preliminary to a measurement the computer performs a several-step test for independence of sampled elements in order to set the sampling frequency The principle of this is that the computer reduces by half the frequency of the sample signal supplied by a variable frequency signal generator whenever the test yields a negative result, and the procedure is continued until the sample elements show an adequately significant independence [2.5].

In the test the computer compares the values of the N elements sampled at the given frequency, writing /+1/ if the measured value of x_i is higher, /-1/ if it is lower, than the expected value $\bar{x}$ [2.6]. The set of /+1/ and /-1/ elements so obtained is then broken up into "runs" of adjacent sample elements having the same sign /see Fig. 2.4/. If the sample elements are truly independent, the expected number of runs is

$$m = \frac{N}{2} + 1$$

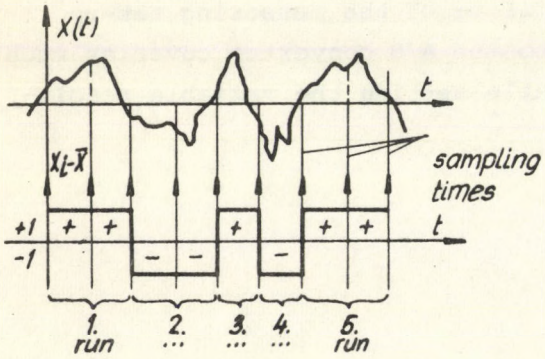

Fig. 2.4

Example of an independence test on computer

The square of the standard deviation is

$$\sigma^2 = \frac{N(N-2)}{4(N-1)} \qquad /2.11/$$

For a prescribed significance, a lower and an upper limit on the number of runs can thus be determined once σ and m are known.

The sampling frequency in the measuring phase is satisfactory if the number of runs obtained from the "run test" falls within the range defined by the calculated limits.

2.6 References

[2.1] A. RÉNYI: Some new criteria for the comparison of two samples /in Hungarian/
MTA Alk.Mat.Tud.Közleményei 243-57 /1954/

[2.2] M.G. KENDELL - A. STEWART: The Advanced Theory of Statistics 2nd Edition, Charles Griffin Co. Ltd., London, 1967.

[2.3] A. RÉNYI: Probability Calculation /in Hungarian/
Tankönyvkiadó, Budapest, 1968

[2.4] F. SZLÁVIK: IAEA Progress Report, October, 1971. Contr.Number 855/R1/RB

[2.5] G. KOZMANN - F. SZLÁVIK: Some problems of system diagnosis from ordered statistical samples /in Hungarian/
Mérés és Automatika /Measurement and Automation/ vol.XX.No.2

[2.6] J. BENDAT - A. PIERSOL: Measurement and Analysis of Random Data /John Wiley & Sons, New York, 1968/

3. THEORETICAL STUDIES OF POWER REACTOR NOISE

EDITED BY G. KOSÁLY*

ABSTRACT

In the present Section we investigate some problems of power reactor noise via a two point model of heat transfer and one point reactor theory.

In Chapter 3.1 the reactor response to inlet temperature fluctuations has been studied. It is shown that a peak which was predicted in the literature does not exist. The sink structure of the transfer function is examined in detail.

In Chapter 3.2 the influence of inlet coolant temperature fluctuations and random mechanical vibrations of a control rod on the power spectral density of neutronic fluctuations has been studied. Using a physically reasonable expression for the power spectral density of the vibrations of the control rod and some results obtained by Robinson [3.7] for the inlet coolant temperature fluctuations, we are able to explain the interesting resonance like structure observed in experimental measurements of the power spectral density of the Oak Ridge Research Reactor /ORR/. We obtain estimates of the root mean square temperature fluctuations and also data connected with the vibration of the control rod.

In Chapter 3.3 the cross correlation function between coolant temperature fluctuations at two different axial positions is calculated. The behaviour of the correlation function is explained for different values of the relevant parameters.

---

* Acknowledgement

Editor is indebted to Prof. A.I. Mogilner /Institute for Physics and Energetics, Obninsk, U.S.S.R./ and to Prof. M.M.R. Williams /Queen Mary College, London, U.K./ for many clarifying discussions on the topic of power reactor noise. Professor Williams was also coauthor of the work dealing with the neutron noise induced by mechanical vibrations and inlet temperature fluctuations. The participation in the work of L.Meskó /CRIP, Budapest, Hungary/ is also acknowledged.

INTRODUCTION

The current effort in reactor noise analysis is undoubtedly being directed towards a better understanding of noise sources in power reactors. This is certainly understandable, since, whilst zero power fluctuations yield interesting information about a reactor system, it is clear that if reactor noise is to have any real future in nuclear engineering it must lead to results of practical engineering value. Thus it must either be of aid in diagnosing existing faults or, better still, help predict these faults before they become serious. Recent reviews by Uhrig [3.1] and Seifritz and Stegemann [3.2] give a very clear picture of the state of the art of noise analysis. From this review we can deduce that zero power problems are rather well understood and only mathematical difficulties remain. On the other hand the problem of noise analysis in power reactors is in its infancy due, mainly, to a lack of basic knowledge of the many noise mechanisms involved.

In this situation it is especially important to perform theoretical investigations parallel to experimental studies.

It is to be noted that theoretical work in the field of reactor noise has strong tradition in our Institute. In this context we refer to the works of L.Pál [3.3] which are still one of the most frequently quoted papers in theoretical studies of zero-power reactor noise.

Following this tradition and prompted by the experimental work in recent years we started to study some problems of power reactor noise. In the present section we report on some of the results of the theoretical investigation.

3.1 Remarks on the transfer function relating inlet temperature fluctuations to neutron noise [3.4]

Inlet temperature fluctuations as a possible source of neutron noise have been considered by several authors.

Boardman [3.5] and Mirsoyan [3.6] allege that certain peaks in their measured spectra can be identified as peaks of the transfer function relating temperature fluctuations at the inlet to neutron noise.

Robinson [3.7] computed this transfer function for the actual case of the Oak Ridge Research Reactor. It is an interesting result of Robinson that in his computed spectra there are clearly visible sharp sinks at frequencies related to the inverse of the transfer time of the coolant through the core. While Robinson attacked the problem in a purely numerical

way, in this chapter we intend to examine more rigorously the peak and sink structure of the transfer function in question.

We let $\vartheta_c(t,z)$ denote the fluctuation in the temperature of the coolant at a distance z from the inlet, and let $\vartheta_f(t,z)$ denote the fuel temperature.

Then using the axial dependent two-point model of heat transfer [3.5], [3.8] we write

$$C_f \frac{\partial \vartheta_f(t,z)}{\partial t} = -h\left[\vartheta_f(t,z) - \vartheta_c(t,z)\right] + p(t)\,\phi(z) \qquad /3.1.1/$$

$$C_c \frac{\partial \vartheta_c(t,z)}{\partial t} = h\left[\vartheta_f(t,z) - \vartheta_c(t,z)\right] - C_c\, V \frac{\partial \vartheta_c(t,z)}{\partial z}$$

where

C_f is the thermal capacity of fuel per unit length,
C_c is the thermal capacity of coolant per unit length,
V is the coolant velocity,
h is the heat-transfer coefficient per unit length,
$\phi(z)$ is the axial flux shape, that is

$$\phi(z) = \cos\left[B\,(z-z_o)\right] \qquad /3.1.2/$$

z_o is the half length of the core and B is the axial buckling.

Following Boardman [3.5] we take the Fourier transforms of Eqs. /3.1.1/. Denoting by $\vartheta_f(\omega,z)$ and $\vartheta_c(\omega,z)$ the Fourier transforms of the fluctuations we have

$$\vartheta_f(\omega,z) = K(\omega)\left[\vartheta_c(\omega,z) + \frac{1}{h}\,p(\omega)\,\phi(z)\right] \qquad /3.1.3a/$$

$$\vartheta_c(\omega,z) = e^{-\beta(\omega)(z-z_1)}\,\vartheta_c(\omega,z_1) +$$

$$+ \frac{p(\omega)\,K(\omega)}{C_c\,V}\, e^{-\beta(\omega)z} \int_{z_1}^{z} e^{\beta(\omega)z'}\,\phi(z')\,dz' \qquad /3.1.3b/$$

Here

$$K(\omega) = \frac{\alpha_f}{\alpha_f + i\omega} \qquad /3.1.4/$$

$$\beta(\omega) = \frac{\alpha_c}{V}\left[1 - K(\omega)\right] + i\,\frac{\omega}{V} \qquad /3.1.5/$$

and

$\alpha_f = \frac{h}{C_f}$, $\alpha_c = \frac{h}{C_c}$ stand for the characteristic frequencies of fuel and coolant, respectively /reciprocals of the time constants τ_f and τ_c/.

With the coolant flowing upwards, in Eqs. /3.1.3a, b/ one has $z \geq z_1$. Both z and z_1 are inside the core that is between $z = 0$ and $z = 2z_o$. In the special case of $z_1 = 0$, Eqs. /3.1.3a, b/ describe the propagation of inlet temperature fluctuations through the core.

$\beta(\omega)$ is the complex frequency dependent spatial attenuation constant of the temperature fluctuations. Using Eqs. /3.1.4/, /3.1.5/ one has

$$\beta(\omega) = \mathrm{Re}\beta(\omega) + i\,\mathrm{Im}\beta(\omega)$$

$$\mathrm{Re}\beta(\omega) = \frac{\alpha_c}{V}\,\frac{\omega^2}{\omega^2 + \alpha_f^2}$$

$$\mathrm{Im}\beta(\omega) = \frac{\omega}{V}\left[1 + \frac{C_f}{C_c}\,\frac{\alpha_f^2}{\alpha_f^2 + \omega^2}\right]$$

In Eq. /3.1.3b/ the first term discribes the direct propagation of the temperature signal through the axial distance $z - z_1$. The second term represents the effect of power fluctuations.

According to point reactor theory the fluctuation in power responding to a known small reactivity fluctuation is given by the equation [3.2]

$$p(\omega) = P_o\, G_o(\omega)\, \Delta\rho(\omega) \qquad /3.1.7/$$

Here P_o stands for the power level of the reactor, $G_o(\omega)$ is the zero-power reactivity transfer function and $\Delta\rho(\omega)$ is the fluctuation of reactivity in the frequency domain.

Using Eqs. /3.1.7/ and /3.1.3a, b/ and relating the reactivity fluctuation to the axial average of the temperature fluctuations via the temperature coefficients of fuel and coolant /μ_f and μ_c/ respectively one obtains that [3-5]

$$p(\omega) = P_o\, G(\omega)\left[\mu_c + \mu_f\, K(\omega)\right] F(\omega)\, \vartheta_c(\omega, z_1 = 0) \qquad /3.18/$$

Here $\vartheta_c(\omega, z_1 = 0)$ is the temperature fluctuation at the core-

inlet, $G(\omega)$ is the power-reactor transfer function [3.2]. $K(\omega)$ is given in Eq. /3.1.4/ and for $F(\omega)$ one obtains that [3.5]

$$F(\omega) = \tilde{F}(\beta) = \frac{A(\beta)}{\beta\left(\beta^2 + 4B^2\right)} \qquad /3.1.9a/$$

$$A(\beta) = \frac{B}{2Bz_o + \sin(2Bz_o)} \left\{ \left(1 - e^{-2Bz_o}\right)\left(4B^2 + \beta^2\left[1 + \cos(2Bz_o)\right]\right) + \right.$$

$$\left. + \left(1 + e^{-2Bz_o}\right) 2\beta\, B \sin(2Bz_o) \right\} \qquad /3.1.9b/$$

The above result was given by Boardman [3.5] and Robinson [3.7]. In the present chapter we concentrate on the examination of the structure of the function $F(\omega)$[x/].

On the first Florida Conference Boardman [3.5] argued that at $\beta = \pm 2iB$ the function $\tilde{F}(\beta)$ has poles leading to a resonance behaviour of the function $F(\omega)$. In his paper he gave expressions relating the location and the width of the resonances to the parameters of the reactor. Using these expressions he identified a strong resonance found in the measured spectrum of the neutron noise of the Dounreay Fast Reactor as caused by one of the aforementioned poles of the function $F(\omega)$.

The results of Boardman were used later by Mirsoyan [3.6] who analysed the neutron noise in the water moderated, water cooled TES-3 reactor. He again interprets a strong peak in his measured spectrum as caused by the structure of the function $F(\omega)$, thereby identifying inlet temperature fluctuations as a major source of neutron noise in the TES-3 reactor. Using measured values for the location and the width of the resonance he calculates the values of the heat transfer coefficient and the flow velocity. The results are claimed to agree well with the values estimated earlier on different grounds.

In contrast to all these speculations we would like to stress that the function $\tilde{F}(\beta)$ is regular at $\beta = \pm 2iB$.

In their considerations Boardman and Mirsoyan did not take into account that at $\beta = \pm 2iB$ besides the denominator of $\tilde{F}(\beta)$ its numerator vanishes as well. In fact simple algebra shows that

---

x/ The other factors in Eq. /3.1.8/ are normally smooth functions of the frequency.

$$A\left(\beta = \pm 2iB\right) = 0 \qquad /3.1.10/$$

Starting from Eq. /3.1.10/ the regularity of the function can be easily proved. The function $|F(\omega)|$ decreases monotonly at the predicted peak frequencies /see Figs. 3.1a, 3.1b where the arrows point to the frequencies of the missing resonances. The resonance frequencies were calculated using the expression given in Ref. [3.5]/.

At the same time the function $F(\omega)$ exhibits a characteristic sink structure determined by the roots of its numerator [3.7]. The physical explanation of this sink structure lies in the integral character of the reactivity of a reactor. The reactivity noise induced by inlet temperature fluctuations vanishes for certain frequencies for which the axial average of the temperature fluctuations equals to zero.

Using the notation

$$R = \frac{1}{1 + \frac{d}{z_o}}$$

where d is the reflector saving in the axial direction and z_o is the half length of the core, direct calculation shows that the equation

$$A(\beta) = 0 \qquad /3.1.11/$$

is solved by the β_n values:

$$\beta_n = 2iBn\left\{1 + \frac{\pi^2}{6}(n^2-1)(R-1)^3 + O\left[(R-1)^4\right]\right\} \qquad /3.1.12/$$

$$B = \frac{\pi}{2z_o + 2d} \qquad n = 2,3,...$$

To find out whether the above zeros* can be observed in the frequency dependence of the function $F(\omega)$ one has to solve the equation

$$\beta(\omega) = \beta_n \qquad /3.1.13/$$

Let $\bar{\omega}_n (n = 2,3,...)$ denote the roots of Eq./3.1.13/. At these in

---

* In fact besides β_n, the value $-\beta_n$ is a root of Eq. /3.1.11/ as well. We do not consider these latter roots as they lead to non-physical solutions /negative frequencies/. The value $n = 1$ was not considered either, as $F(\beta)$ remains finite for $\beta = \beta_1$.

general complex frequencies the function $F(\omega)$ has zeros on the complex ω-plane. These zeros will lead to clearly visible, sharp sinks at the real frequencies

$$\omega_n = \mathrm{Re}\ \bar{\omega}_n \qquad /3.1.14/$$

if

$$\mathrm{Re}\ \bar{\omega}_n > 0 \qquad /3.1.15a/$$

and

$$\mathrm{Re}\ \bar{\omega}_n >> |\mathrm{Im}\ \bar{\omega}_n| \qquad /3.1.15b/$$

Inspection of Eqs. /3.1.6/, /3.1.12/ and /3.1.13/ shows that the condition given in Eq. /3.1.15b/ is equivalent to

$$\frac{\alpha_c}{2VBn} \frac{\omega_n^2}{\omega_n^2 + \alpha_f^2} << 1 \qquad /3.1.16/$$

Using Eqs. /3.1.6/, /3.1.16/ and /3.1.12/ in Eq. /3.1.13/ leads to

$$\omega_n = \frac{2V\ B\ n}{1 + \frac{C_f}{C_c} \frac{\alpha_f^2}{\omega_n^2 + \alpha_f^2}} \qquad /3.1.17/$$

Eq. /3.1.17/ gives the sink-frequencies of the function $F(\omega)$, that is the frequencies of the sinks appearing in the spectrum of cross correlation between inlet temperature fluctuations and neutron noise. Eq. /3.1.16/ is the condition of the visibility of the sinks.

Trying to solve Eq. /3.1.17/ by successive approximation and taking 2VBn as the solution in the zeroth order one finds that in many cases

$$\frac{C_f}{C_c} \frac{\alpha_f^2}{4V^2\ B^2\ n^2 + \alpha_f^2} << 1 \qquad /3.1.18/$$

that is the sink frequencies are given by the simple expression

$$\omega_n \simeq 2V\ B\ n \quad , \quad n = 2,3,... \qquad /3.1.19/$$

If $d << z_o$, then $B \simeq \frac{\pi}{2z_o}$ leading to

$$\omega_n \simeq 2\pi \frac{V}{2z_o} n = \frac{2\pi}{\tau} n \qquad n = 2,3,... \qquad /3.1.20/$$

where τ is the transfer time of the coolant through the core [3.7].

WWR-SM

$T_{inlet} = 40°C$
$W = 0{,}5\,MW$

$\frac{V}{(m/s)}$	$\frac{\alpha_c}{4VB} \cdot \frac{4\pi^2 f_2^2}{4\pi^2 f_2^2 + \alpha_f^2}$	f_2 (cps)	$\frac{2VB}{\pi}$ (cps)
1,0	0,056	2,62	2,67
2,0	0,049	5,24	5,34
3,0	0,045	7,86	8,01

Table 3.1a

Values of the first sink frequency for the WWR-SM reactor. In the first columm the quantity characterizing the sharpness of the sink is given (see Eq./3.1.16/).

ORR

$T_{inlet} = 40°C$
$W = 4{,}8\,MW$

V (m/s)	$\frac{\alpha_c}{4VB} \cdot \frac{4\pi^2 f_2^2}{4\pi^2 f_2^2 + \alpha_f^2}$	f_2 (cps)	$\frac{2VB}{\pi}$ (cps)
1,0	0,013	2,52	2,56
2,0	0,012	5,03	5,12
3,0	0,011	7,55	7,68

Table 3.1b

Values of the first sink frequency for the ORR reactor. In the first columm the quantity characterizing the sharpness of the sink is given (see Eq./3.1.16/)

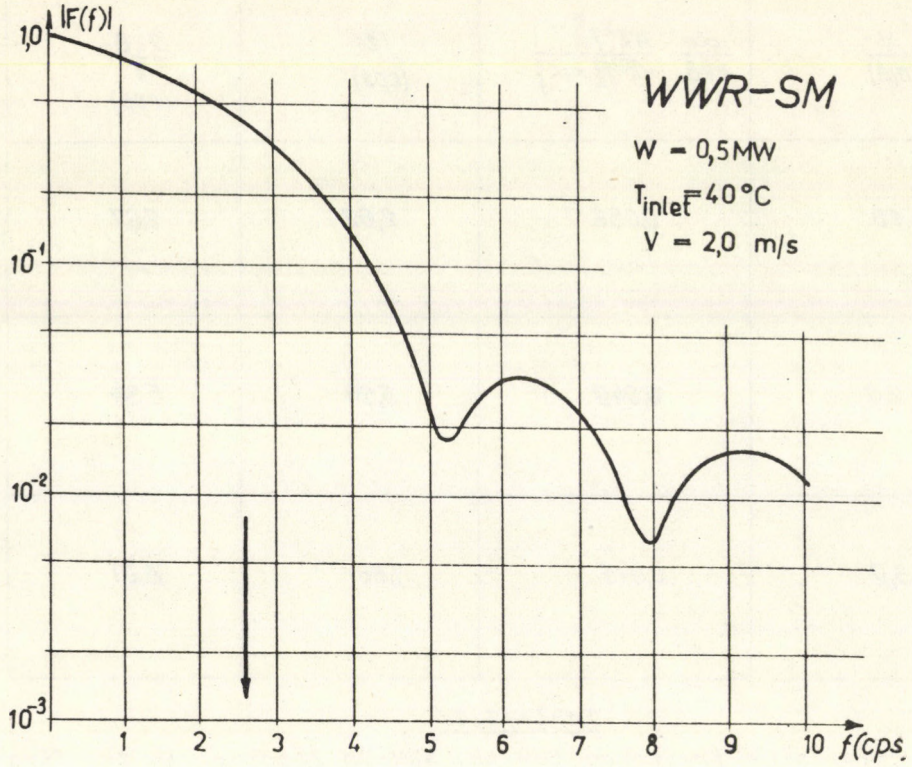

Fig. 3.1a

The function |F(f)| for the WWR-SM reactor

In Tables 1a and 1b the locations of the first sink are given for the WWR-SM reactor and for the Oak Ridge Research Reactor, respectively. In the second column of the tables the exact values of the sink frequencies f_2 are given as read from the computed curves of |F(f)|. Comparing them with the values given by Eq. /3.1.19/ one sees that the agreement is rather good.

Figures 3.1a and 3.1b show the function |F(f)| for the WWR-SM reactor, and for the Oak Ridge Reactor respectively, for the flow velocity V = 2m/s. The sinks are much sharper for the ORR than for the WWR-SM. This behaviour is explained by the first column of the Tables.

The arrows on the Figures point to the frequencies of the supposed resonances [3.5], [3.6] mentioned above. The function decreases monotonly in this region.

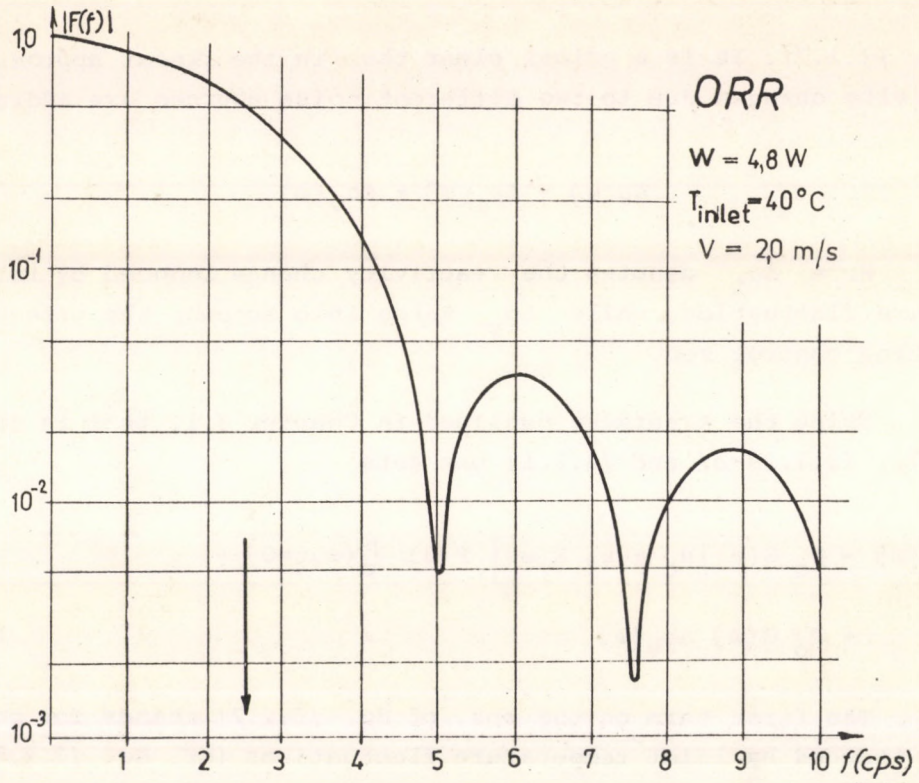

Fig. 3.1b

The function $|F(f)|$ for the ORR reactor

The above considerations show that the transfer function relating temperature fluctuations to power fluctuations exhibits a characteristic sink-structure. At the same time it was shown that a peak which was predicted in the literature does not exist.

At the same time it is to be noted that between neighbouring sink there are necessarily peaks having a different origin and location than the non-existing one which has been predicted. As the frequencies of the sinks move approximately linearly with increasing velocity the location of the latter peaks will move with changing velocity of the coolant as well.

In this context one should remember that velocity dependent peak frequencies have been found in several neutron noise measurements [3.10]. One may speculate that fluctuating inlet temperature as a noise source might be the explanation of the phenomenon in certain cases.

3.2 Point theory of the neutron noise induced by temperature fluctuations and random vibrations of a control element [3.11]

According to point reactor theory the fluctuation of power is given

by Eq. /3.1.7/. It is a priori clear that in the linear approximation the reactivity changes due to two different noise sources are additive that is

$$\Delta\rho(\omega) = \Delta\rho_i(\omega) + \Delta\rho_v(\omega) \qquad /3.2.1/$$

Here $\Delta\rho_i$ denotes the reactivity change induced by inlet temperature fluctuation, while $\Delta\rho_v$ takes into account the effect of a vibrating control rod.

Using the treatment outlined in Chapter 3.1, that is using Eqs. /3.1.7/, /3.1.3a-b/ and /3.2.1/ one gets

$$p(\omega) = P_o\, G(\omega)\left[\mu_c + \mu_f\, K(\omega)\right] F(\omega)\, \vartheta_c(\omega, z=0) +$$

$$+ P_o\, G(\omega)\, \Delta\rho_v(\omega) \qquad /3.2.2/$$

The first term on the rhs. of Eq. /3.2.2/ stands for power fluctuations induced by inlet temperature fluctuations (cf. Eq. /3.1.8/), the second term is the contribution of mechanical vibrations. $G(\omega)$ is the power-reactor transfer function [3.2].

Now the reactivity fluctuation induced by random mechanical vibrations is to be analysed. Consider the case of a slab reactor having vacuum boundaries at $x = \pm a$. At $x = x_o$ an infinitely thin absorbing plate is imbedded in the reactor.

For the case of equilibrium we use the static reactor equation in the one group diffusion approximation:

$$\left(\frac{1}{K_{eff,o}}\,\hat{P} - \hat{D} - \hat{S}_o\right)\phi_o(x) = 0 \qquad /3.2.3/$$

While $\hat{P}$ and $\hat{D}$ are the well known production and destruction operators of the homogenised reactor, the operator $\hat{S}_o$ stands for the effect of the absorbing plate.

$$\hat{S}_o = \gamma\, \delta(x - x_o) \qquad /3.2.4/$$

The parameter γ is Galanin's constant characterizing the strength of the infinitely thin absorber.

In the above equations the quantities carrying the subscript "o" are related to the equilibrium situation. With the commencement of vibration of the plate these quantities will change.

Since in one group diffusion theory the adjoint function is equal to the static flux, the reactivity of the equilibrium reactor can be written in the following well known form:

$$\rho_o = 1 - \frac{1}{K_{eff,0}} =$$

$$= \frac{\int_{-a}^{+a} \phi_o(x)\, \hat{P}\, \phi_o(x)\, dx - \int_{-a}^{+a} \phi_o(x)\, \hat{D}\, \phi_o(x)\, dx - \int_{-a}^{+a} \phi_o(x)\, \hat{S}_o\, \phi_o(x)\, dx}{\int_{-a}^{+a} \phi_o(x)\, \hat{P}\, \phi_o(x)\, dx} \qquad /3.2.5/$$

If the plate executes vibrations, all terms in Eq. /3.2.5/ become time dependent, leading to a time dependence of the reactivity. As the operators $\hat{P}$ and $\hat{D}$ in the first order do not change with the vibration of the plate, the time dependence of the reactivity originates from the time dependence of the flux, and from the time dependence of the operator characterizing the plate itself. In perturbation theory it is proved that the above expression of reactivity is stationary in the flux, thus in the first order, the change of reactivity is caused exclusively by the change of the operator $\hat{S}_o$ to its non-equilibrium value $\hat{S}(t)$. Following Williams [3.12] we write

$$\hat{S}(t) = \gamma\, \delta\left[x - x_o - \varepsilon(t)\right] \qquad /3.2.6/$$

where $\varepsilon(t)$ denotes the displacement of the plate from its equilibrium position at time t. In the linear theory one uses

$$\hat{S}(t) = \hat{S}_o - \gamma\, \varepsilon(t)\, \delta'(x - x_o) \qquad /3.2.7/$$

rather than the exact form. If in Eq. /3.2.5/ $\hat{S}_o$ is replaced by the operator given in Eq. /3.2.7/ the following result is obtained for the reactivity fluctuation driven by plate vibrations:

$$\rho(t) - \rho_o \simeq \Delta\rho_v(t) = \varepsilon(t)\,\gamma\,\frac{\int_{-a}^{+a} \delta'(x-x_o)\,\phi_o^2(x)\,dx}{\int_{-a}^{+a} \phi_o(x)\,\hat{P}\,\phi_o(x)\,dx} =$$

$$= \varepsilon(t)\,\gamma\,\frac{\int_{-a}^{+a} \phi_o^2(x)\,dx}{\int_{-a}^{+a} \phi_o(x)\,\hat{P}\,\phi_o(x)\,dx} \cdot \frac{\int_{-a}^{+a} \delta'(x-x_o)\,\phi_o^2(x)\,dx}{\int_{-a}^{+a} \phi_o^2(x)\,dx}$$

Thus in the first order

$$\Delta\rho_v(t) = A\,\gamma\,\Lambda\,\varepsilon(t) \qquad /3.2.8/$$

Here Λ is the neutron generation time while

$$A = \frac{\phi_o(x_o)}{\int_{-a}^{+a} \phi_o^2(x)\,dx} \lim_{\mu \to +o} \left[\left(\frac{\partial \phi_o}{\partial x} \right)_{x_o+\mu} + \left(\frac{\partial \phi_o}{\partial x} \right)_{x_o-\mu} \right]$$

Using Eq. /3.2.8/ in Eq. /3.2.2/ the auto-spectral density of the power fluctuations can be easily expressed by the auto-spectral densities of the noise-sources in question.

$$\phi_p(\omega) = P_o^2 |G(\omega)|^2 \, |\mu_c + \mu_f\, K(\omega)|^2 \, |F(\omega)|^2 \, \phi_i(\omega) +$$

$$+ P_o^2 |G(\omega)|^2 \, \gamma^2 A^2 \Lambda^2 \, \phi_v(\omega) \qquad /3.2.9/$$

Here

$$\phi_p(\omega) = \langle p^*(\omega)\, p(\omega) \rangle$$

$$\phi_i(\omega) = \langle \vartheta_c^*(\omega,o)\ \vartheta_c(\omega,o) \rangle$$

$$\phi_v(\omega) = \langle \varepsilon^*(\omega)\, \varepsilon(\omega) \rangle$$

It is well known that high velocity coolant flowing through the reactor core is a source of energy that can induce and sustain vibration in the reactor core components. While the vibrations of mechanical elements attached to motionless supports is a common noise-source in all reactors at-power, from the point of view of reactor diagnostics the pathological case

of excess vibrations due to some failures in the supports seems to be more important. In particular, if the bar is held by bearings then following the failure of the bearings at one end, an extremely complicated motion of the bar might be induced by turbulent flow. While this motion is rather complicated it can be surely described approximately as a motion dominated by a single frequency /basically the frequency of the bowing of the rod in the slight clearance at the defective end/ and damping. Thus we write the auto-spectral density of vibrations as [3.13]:

$$\phi_v(\omega) = \Delta^2 \left[\frac{K}{(\omega_o-\omega)^2 + K^2} + \frac{K}{(\omega_o+\omega)^2 + K^2} \right] \qquad /3.2.10/$$

Here ω_o is the characteristic frequency of the motion and K stands for damping

$$\Delta^2 = \langle \varepsilon^2 \rangle$$

The above formulae form a basis for the theoretical treatment of power fluctuations induced by inlet temperature fluctuations and random mechanical vibrations of a control element.

Discussing the measurements of Stephenson, Roux and Fry [3.14] it is claimed in Ref. [3.7] that the strong peak observed in the noise spectrum of the Oak Ridge Research /ORR/, was due to excessive vibrations following the failure of the upper bearing of one of the shim roads. The appearance of similar peaks following failures of shim-rod-bearings have been observed by Fry and Robinson [3.15] in the noise spectrum of the High Flux Isotope Reactor. Now we try to use the spectral density given in Eq. /3.2.9/ together with the vibrational spectrum given in Eq. /3.2.10/ for the interpretetion of the noise spectrum of the ORR. For the inlet temperature fluctuations the assumption of white-noise will be used.

Fig. 3.2 shows the experimental power spectra of neutron density fluctuations as given in Ref. [3.7]. From the data given by Stephenson, Roux and Fry [3.14] the correlated background has been subtracted and the result has been divided by the dc current squared. Using the notations of the present paper, Fig. 3.2 gives the observed values of the quantity $1/P_o^2\ \phi_p(f)$ versus frequency. Fig. 3.3 and 3.4 show the functions $|G(f)|^2$ and $|G(f)[\mu_c + \mu_f K(f)]F(f)|^2$ respectively as calculated for the ORR by Robinson [3.7].

According to Robinson [3.7] the peaks which can be seen in the experimental curves are caused by the failure of the upper-shim-rod-bearing leading to excessive vibrations of the rod. In view of the results in the

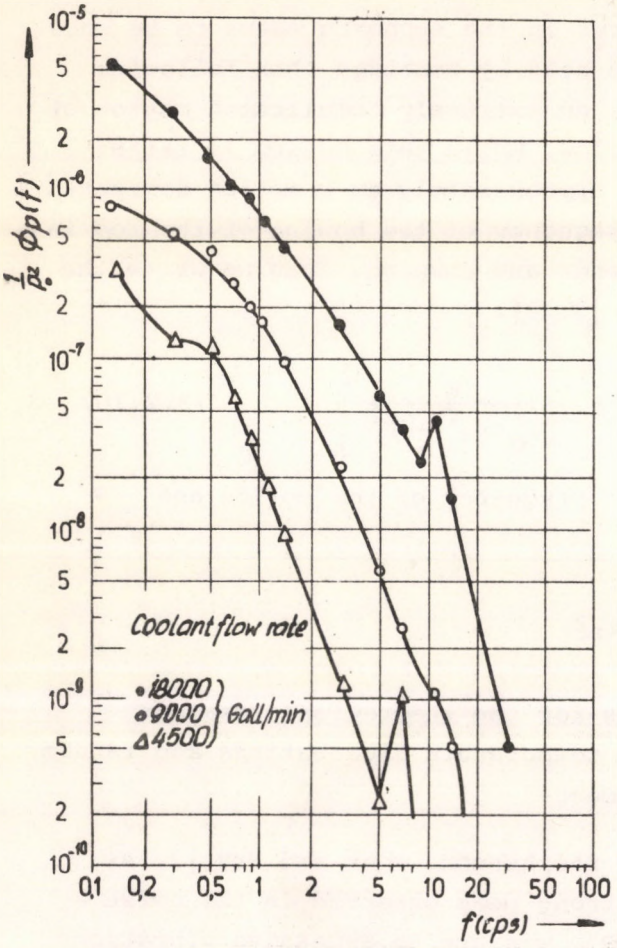

Fig. 3.2

Experimental power spectra for the ORR at different coolant flow rates at 3,75 MW (see Fig. 6 in Ref. [3.7])

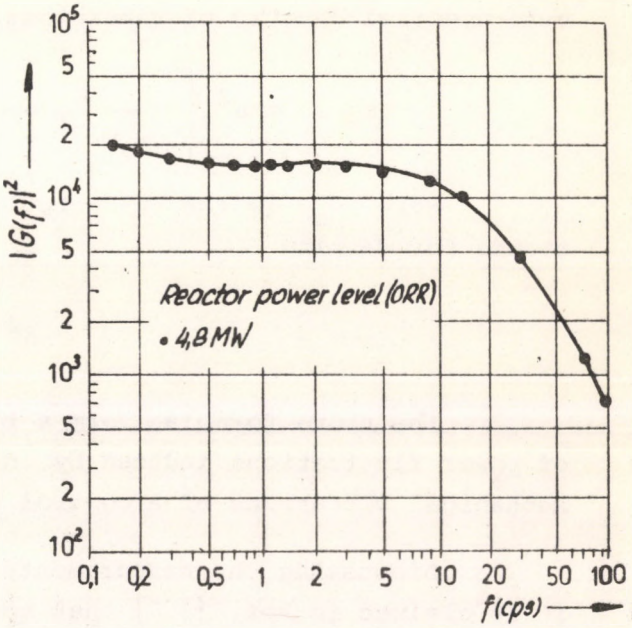

Fig. 3.3

Calculated power spectra density for the ORR at 4,8 MW with a white reactivity driving function of unity magnitude see (Fig. 7. in Ref. [3.7])

last section the power spectrum density of these vibrations is given approximately by Eq. /3.2.10/. The frequency and the damping of the motion might depend on the flow velocity. This dependence manifests itself in the experimental results by the shift of the location of the peak with increasing flow velocity. For the flow rate 9000 gpm the peak disappears and only some traces of an inflexion can be seen at about 10 Hz.

While the presence of the peak in the experimental spectra can be explained by excessive mechanical vibrations, the strong ascendance of the spectra towards decreasing frequencies at the left hand side of the peaks cannot be understood without invoking other possible noise sources.

A detailed comparison of Fig. 3.2 and Fig. 3.4 shows that for all flow velocities there is a region in the left hand side vicinity of the peaks /or in the left hand side vicinity of the elbow for medium flow rate/

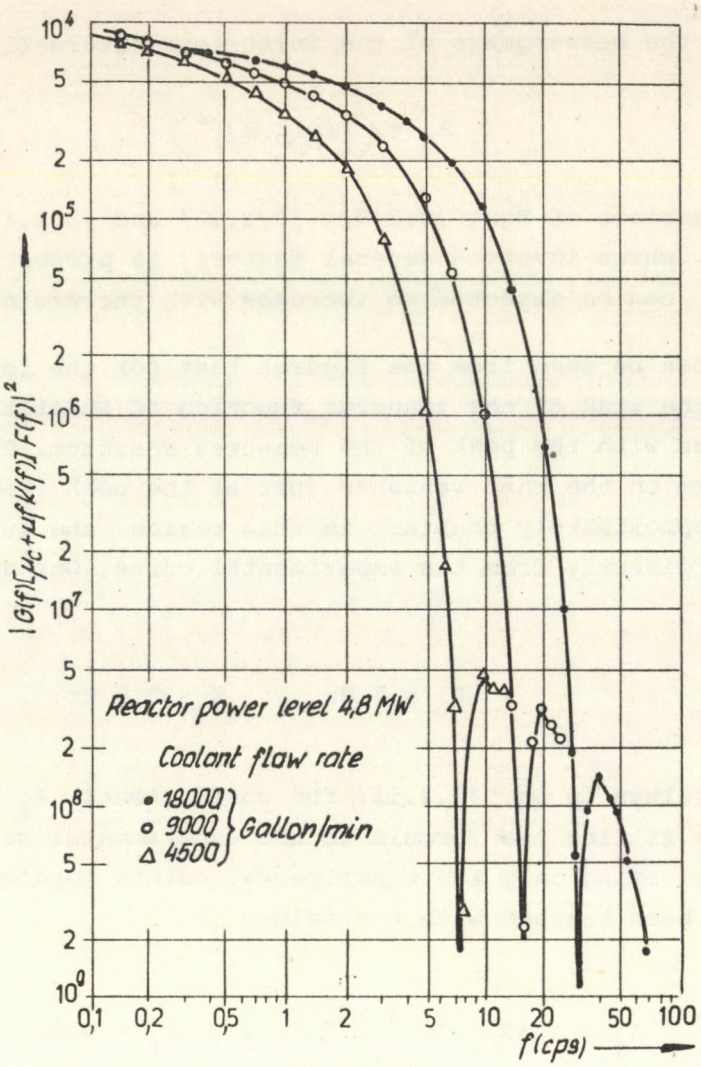

Fig. 3.4

Calculated power spectral density for the ORR at 4,8 MW for a white inlet temperature fluctuation driving function (see Fig.9, in Ref. [3.7])

where the experimental spectrum is parallel to the function $|G(f)[\mu_c + \mu_f K(f)]F(f)|^2$ corresponding to the same flow velocity. This indicates that, in these reqions, white inlet-temperature fluctuations might be the dominating noise-source.

On the basis of these facts we will attempt to fit the experimental curves with the formula

$$\frac{1}{P_o^2}\,\phi_p(f) = \left|G(f)\left[\mu_c + \mu_f\, K(f)\right]\, F(f)\right|^2 A_i + \\ + |G(f)|^2 \left[\frac{K}{(F_o-f)^2 + K^2} + \frac{K}{(F_o+f)^2 + K^2}\right] A_v \qquad /3.2.11/$$

Here A_i is the mean-square of the inlet-temperature fluctuation, that is

$$A_i = \left\langle \left[\vartheta_c(t,0) \right]^2 \right\rangle \qquad /3.2.12/$$

Comparison of Eqs. /3.2.9/, /3.2.10/ and /3.2.11/ shows that the quantity A_v, which involves several factors, is proportional to the quantity Δ^2, thus A_v can be expected to increase with increasing flow velocity.

It can be seen from the figures that for the lowest flow rate the location of the sink of the transfer function of inlet temperature fluctuation coincides with the peak of the measured spectrum. Thus in Eq. /3.2.11/ the first term on the rhs. vanishes just at the peak frequency and, as $|G(f)|^2$ is approximately constant in this region, the quantities F_o and K can be taken directly from the experimental curve. One gets in this way the values

$$F_o = 7 \text{ Hz} \quad , \quad K = 0{,}6 \text{ Hz}$$

Using these values in Eq. /3.2.11/ the coefficients A_i and A_v can be determined by fitting the formula to the experimental curve by the method of least-squares. Using only the experimental points located at $f \geq 3$Hz the best fit has been reached with the values

$$A_i = 1.47 \cdot 10^{-4} \ (^oF)^2 \quad , \quad A_v = 3.60 \cdot 10^{-14} \ s^{-1}$$

The lower solid curve on Fig. 3.5 shows that, using the above values for the coefficients, the theoretical formula fits extremely well the experimental points at least for $f \geq 3$Hz. If experimental points at lower frequencies are included in the fitting procedure no reasonable fit can be achieved, demonstrating for these frequencies the influence of some noise sources which are neglected in Eq. /3.2.11/.

For the medium flow rate the lack of a clearly visible peak in the experimental spectrum makes it impossible to get F_o and K directly from the curve. Therefore one is forced to determine all of the four parameters (F_o, K, A_i and A_v) from the least square fitting. The best fit has been reached with the values

$$F_o = 11.8 \text{ Hz} \qquad K = 3.5 \text{ Hz}$$

$$A_i = 4.21 \cdot 10^{-4} \ (^oF)^2 \qquad A_v = 2.84 \cdot 10^{-13} \ s^{-1}$$

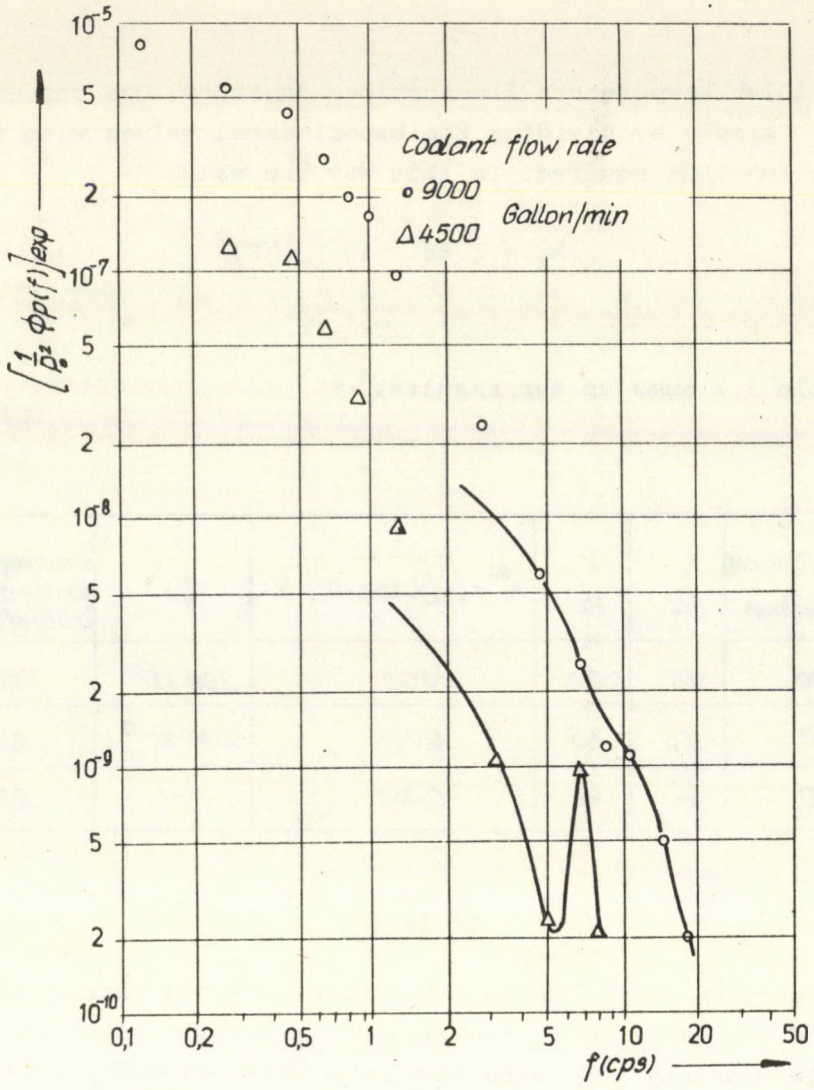

Fig. 3.5

Comparison of the experimental power spectra with the theoretical results. Solid lines show the results obtained by using (Eq./3.2.11/)

The upper solid curve on Fig. 3.5 is the theoretical curve with the above values of the four parameters. Disregarding the experimental point at 8 Hz which was taken as a strayway point the fit is excellent in the region $f \geq 4{,}8$ Hz.

While for the flow rates 4500 gpm and 9000 gpm the experimental curves could be readily fitted in the vicinity of the relevant vibrational frequencies /7 Hz and 11,8 Hz respectively/ for the highest flow rate the method of least squares has not given even a reasonable fit. The authors suspect that the two experimental points at the high frequencies might be erroneous. Thus for this flow rate the quantities F_o, K and A_v cannot be given. At the same time comparison of the experimental curve with the graph of $\left|G(f)\left[\mu_c + \mu_f K(f)\right]F(f)\right|^2$ shows that between 6 Hz and 9 Hz they are parallel to each other indicating that for the flow rate at hand this is the region

where white inlet temperature fluctuations dominate. One can estimate the value of A_i simply by dividing the experimental values with the value of the transfer function squared. In this way the value

$$A_i = 1.88 \cdot 10^{-3} \ (^{o}F)^2$$

is obtained.

Table 3.2 sums up our results.

Coolant flow rate gallon/min	F_o Hz	K Hz	$A_i^{1/2} = \sqrt{\langle [\vartheta_c(t,z=0)]^2 \rangle}$	A_v s^{-1}	Limitfrequency for the applicability of Eq(3.2.11)
4500	7,0	0,6	0,012	$3{,}60 \cdot 10^{-14}$	3,0
9000	11,8	3,5	0,021	$2{,}84 \cdot 10^{-13}$	4,8
18500	—	—	0,043	—	6,0

Table 3.2

Inspection of the table shows that both the characteristic frequency and the damping of the vibration increases with increasing flow velocity. The quantity A_v also increases with the velocity showing that the mean-amplitude of the vibration increases as was expected.

The increase of the RMS of inlet-temperature fluctuations with flow velocity is roughly linear. It is characteristic of the sensitivity of noise measurements that such extremely small temperature fluctuations can be traced in the noise-spectrum.

In the last column of the Table, the limit frequency of the applicability of Eq. /3.2.11/ can be seen. This is the limit frequency above which the neutron noise can be interpreted by random mechanical vibrations of a single element and by white inlet temperature fluctuations. The shift of this limit-frequency with increasing values of the flow velocity indicates that the characteristic frequencies of noise sources other than those considered in the present treatment are also dependent on the coolant velocity

3.3 Investigation of the cross correlation function of coolant temperature fluctuations [3.19]

In recent years several papers have been published reporting on coolant flow velocity determination by the analysis of temperature fluctuations of the coolant [3,16], [3.17], [3.18].

The principle of the method is rather simple. Denoting by $\vartheta_c(t,z)$ the fluctuation of the temperature of the coolant at a distance z from the inlet, one expects on simple physical grounds that

$$\vartheta_c(t,z) = e^{-r\Delta z} \; \vartheta_c\left(t - \frac{\Delta z}{V} \; , \; z_1\right) \qquad /3.3.1/$$

where $\Delta z = z - z_1 \geq 0$ with the coolant flowing upwards in the channel with the average velocity V.

In Eq. /3.3.1/ it is assumed that while the temperature signal is transported downstream by the flowing fluid or gas its amplitude decreases exponentially but its shape does not change.

Using the notations [1]

$$\phi_{z_1,z}(\tau) = \lim_{T\to\infty} \frac{1}{2T} \int_{-T}^{+T} \vartheta_c(t,z_1) \; \vartheta_c(t+\tau,z) \; dt$$

/cross-correlation function between temperature fluctuations at two different axial positions/

$$\phi_{z_1,z_1}(\tau) = \lim_{T\to\infty} \frac{1}{2T} \int_{-T}^{+T} \vartheta_c(t,z_1) \; \vartheta_c(t+\tau,z_1) \; dt$$

/autocorrelation function of the temperature fluctuations at distance z_1 from the inlet/

it follows from Eq. /3.3.1/ that

$$\phi_{z_1,z}(\tau) = e^{-r\Delta z} \; \phi_{z_1,z_1}(\tau) \qquad /3.3.2/$$

As autocorrelation functions are by definition maximal for zero time lag the above cross-correlation function has its maximum at

$$\tau = \frac{\Delta z}{V}$$

Measuring the cross-correlation function of the signals of two thermocouples located at the axial levels z_1 and z respectively, the velocity of the coolant can be evaluated.

Unfortunately the situation is not always as simple as that. On the one hand in a nuclear reactor power fluctuations are always present and their effect to the measurement cannot always be neglected. On the other hand even if power fluctuations give but a negligible contribution to the cross-correlation function, the effects producing the attenuation factor in Eq. /3.3.1/ will also change the shape of the signal, resulting in a more intricate relation between cross-correlation function and auto-correlation function than the one given in Eq. /3.3.2/.

In the present paper we intend to examine the above problems via the axial dependent two-point model of heat transfer [3.8], [3.5].

For this end we start from Eq. /3.1.3b/ writing

$$\phi_c(\omega,z) = e^{-\beta(\omega)(z-z_1)} \vartheta_c(\omega,z_1) \qquad /3.3.3/$$

In Eq. /3.3.3/ z and z_1 denote the position of the upper and lower thermocouple respectively. In Ref. [3.19] the way of an a priori estimation of the feedback effect was demonstrated. Writing Eq. /3.3.3/ the feedback term /second term on the rhs. of Eq. /3.1.3b// has been neglected.

From Eq. /3.3.3/ the relation

$$\phi_{z_1,z}(\omega) = e^{-\beta(\omega)(z-z_1)} \phi_{z_1,z_1}(\omega) \qquad /3.3.4/$$

follows where $\phi_{z_1,z}(\omega)$ and $\phi_{z_1,z_1}(\omega)$ are the cross spectral density and the autospectral density corresponding to $\phi_{z_1,z}(\tau)$ and $\phi_{z_1,z_1}(\tau)$ respectively.

Using Eq. /3.1.5/ for $\beta(\omega)$ one gets that

$$\phi_{z_1,z}(\tau) = \frac{e^{-\gamma}}{2\pi} \int_{-\infty}^{+\infty} e^{i\omega\left(\tau - \frac{\Delta z}{V}\right)} e^{\gamma K(\omega)} \phi_{z_1,z_1}(\omega)\, d\omega \qquad /3.3.5/$$

where $K(\omega)$ was given in Eq. /3.1.4/ and

$$\gamma = \frac{\alpha_c \Delta z}{V} \qquad /3.3.6/$$

is the dimensionless measure of the distance between the two thermocouples.

Assuming the form

$$\phi_{z_1,z_1}(\tau) = e^{-\alpha|\tau|} \qquad /3.3.7/$$

the integral in Eq. /3.3.5/ can be readily evaluated leading to

$$\phi_{z_1,z}(\tau) = e^{-\alpha T}\, e^{\frac{\gamma}{\nu-1}} +$$

$$+ e^{-\alpha T\nu}\, e^{-\gamma}\left\{ \sum_{N=0}^{\infty} \frac{[\alpha T(\nu+1)]^N}{N!} \left[e^{\frac{\gamma\nu}{\nu+1}} - \sum_{\ell=0}^{N} \left(\frac{\gamma\nu}{\nu+1}\right)^{\ell} \frac{1}{\ell!} \right] + \right.$$

$$\left. + \sum_{N=0}^{\infty} \frac{[\alpha T(\nu-1)]^N}{N!} \left[\sum_{\ell=0}^{N} \left(\frac{\gamma\nu}{\nu-1}\right)^{\ell} \frac{1}{\ell!} - e^{\frac{\gamma\nu}{\nu-1}} \right] \right\} \quad , \quad \text{if} \quad T > 0$$

$$\phi_{z_1,z}(\tau) = e^{\alpha T}\, e^{-\frac{\gamma}{\nu+1}} \quad , \quad \text{if} \quad T < 0 \qquad /3.3.8/$$

where the notations

$$T = \tau - \frac{\Delta z}{V}$$

$$\nu = \frac{\alpha_f}{\alpha}$$

have been used.

T measures the deviation of the time lag from the transit time.

For a fixed value of γ one gets that

$$\phi_{z_1,z}(\tau) \approx e^{-\gamma}\, e^{-\alpha\left|\tau-\frac{\Delta z}{V}\right|} \quad , \quad \text{if} \quad \nu << 1 \qquad /3.3.9a/$$

and

$$\phi_{z_1,z}(\tau) \approx e^{-\alpha\left|\tau-\frac{z}{V}\right|} \quad , \quad \text{if} \quad \nu >> 1 \qquad /3.3.9b/$$

Thus the simple relation given in Eq. /3.3.2/ cannot be applied unless the frequencies relevant in the measurement /i.e. the value of the time constant α/ are either much higher (cf.Eq./3.3.9a/) or much lower (cf. Eq./3.3.9b/) than the characteristic frequency α_f of the fuel. In fact the axial attenuation constant r turns out to be frequency dependent. $r = \gamma$ for the high frequency case, and $r = 0$ for the low frequencies.

In the cases between these two extremes no simple relation exists between the autocorrelation function and the cross correlation function but Eq. /3.3.8/ is to be consulted.

The function given in Eq. /3.3.8/ is continuous and maximal at $T = 0$, where its value is given by

$$\phi_{z_1,z}\left(\tau = \frac{\Delta z}{V}\right) = e^{-\frac{\gamma}{\nu+1}} \qquad /3.3.10/$$

With increasing distance between the two thermocouples the value of γ increases, that is the height of the peak decreases [3.18]. The decrease of the height measures the diminution of the correlation as the signal moves along. As a quantitative measure of the correlated part to the uncorrelated part Mika, Raes, and Stegeman [3.18] introduced the ratio S/R where

$$S = \phi_{z_1,z}\left(\tau = \frac{\Delta z}{V}\right)$$

$$R = \phi_{z_1,z}(\tau = 0.) - \phi_{z_1,z}\left(\tau = \frac{\Delta z}{V}\right) \qquad /3.3.11/$$

Using Eq. /3.3.10/ we obtain that

$$\frac{S}{R} = \frac{e^{-\frac{\gamma}{\nu+1}}}{1 - e^{-\frac{\gamma}{\nu+1}}} \qquad /3.3.12/$$

measures the correlation in the present model.

As for turbulent water the velocity dependence of the quantities α_f and α_c is well known / $\sim v^{0,8}$ /, if the velocity dependence of the time constant α of the autocorrelation function is investigated experimentally one might be able to predict whether the height of the peak will increase or decrease with increasing values of the velocity [3.18].

Figs. /3.6a - c/ show the computed curves of the correlation function versus the dimensionless time variable

$$T\alpha = \left(\tau - \frac{\Delta z}{v}\right) \alpha$$

The function $e^{-\alpha|T|}$ is drawn by dashed line. This would be the shape of the correlation function if the fluid flow would transfer the original signal Eq. /3.3.7/ without changing its shape and amplitude. The solid lines show the correlation function for different values of the parameters γ and ν.

For large values of γ the curves differ appreciably from the simple exponential shape. For high and low values of ν the curves behave as dictated by Eq. /3.3.9a/ and Eq. /3.3.9b/ respectively.

The asymmetry of the curves is to be observed on the figures. In fact the correlation is always stronger for $\tau > \frac{\Delta z}{v}$, than for $\tau < \frac{\Delta z}{v}$. This effect is caused by the solid /fuel/ which can store the heat for a while and release it afterwards. The asymmetry increases with the distance between the thermo-couples /characterized by the parameter γ/ and vanishes if the frequencies are much higher or much lower than the characteristic frequency of the fuel.

In the above considerations the axial dependent two point theory of heat transfer was used. The equations of this theory describe the axial transfer of heat by fluid flow and radial heat transfer between fuel and coolant. It is the latter effect which leads to a change of the amplitude and of the time-shape of the signal in this model. As neither the radial dependence of the flow velocity nor the radial dependence of the noise field are taken into account in the model, the smearing effects related to this dependence were not considered in the present work.

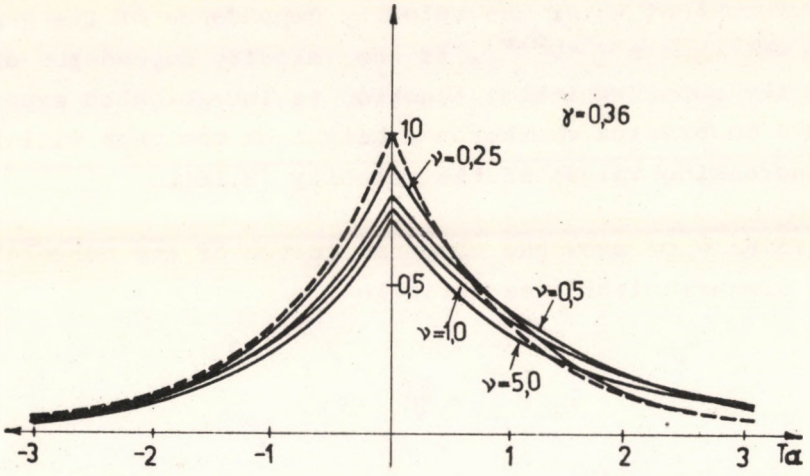

Fig. 3.6a

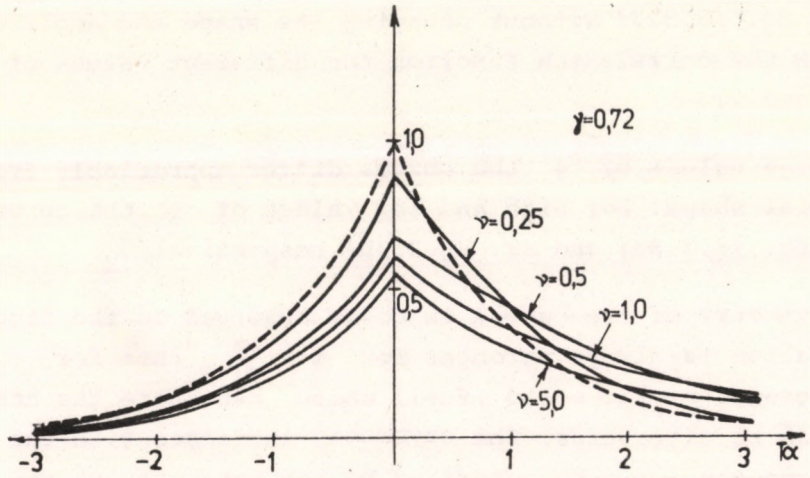

Fig. 3.6b

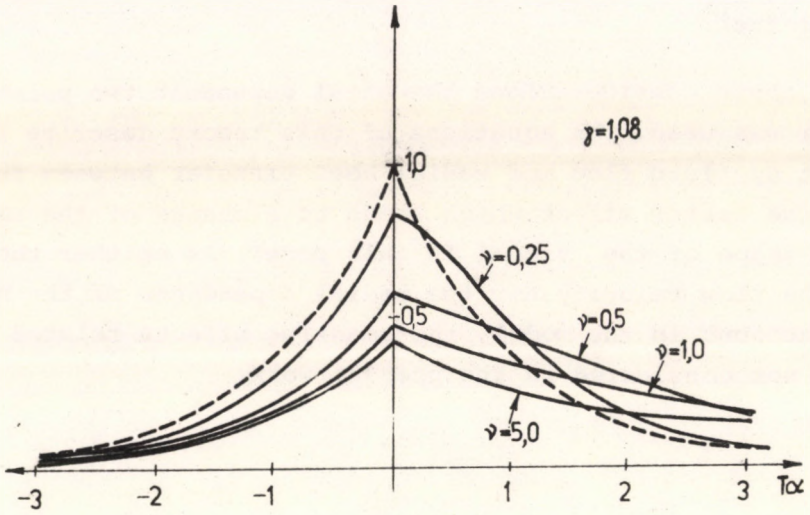

Fig. 3.6c

The cross correlation function versus the dimensionless time variable $T\alpha . T = \tau - \frac{\Delta z}{v}$ *measures the deviation of the time lag from the transit time between the two thermocouples*

3.4 References

[3.1] UHRIG, R.E.: Random Noise Techniques in Nuclear Reactor Systems. The Ronald Press Company, New-York /1970/.

[3.2] SEIFRITZ, W., and D. STEGEMANN: Reactor Noise Analysis, Atomic Energy Review 9, 129 /1971/.

[3.3] PÁL, L., Nuovo Cimento Suppl. VIII. 25 /1958/
PÁL, L.,: "Statistical fluctuations of neutron multiplication" Int.Conf.Peaceful Usis of Atomic Energy /Proc. Conf.Geneva 1958/ 16, UN, Geneva 687 /1958/
PÁL, L., Acta Physica Hungarica 14, 345, 356, 369 /1962/
PÁL, L., J. Nucl. Energy, Parts A/B 17, 395 /1963/

[3.4] KOSÁLY, G., L. MESKÓ: "Remarks on the Transfer Function Relating Inlet Temperature Fluctuations to Neutron Noise". Submitted for publication to the Atomkernenergie.

[3.5] BOARDMAN, F.D.: Noise Measurements in the Dounreay Fast Reactor. Noise Analysis in Nuclear Systems, Gainesville, Florida, Nov. 4-6, 1963, AEC Symposium Series No.4 TID-7679, U.A. Atomic Energy Commission /1964/

[3.6] MIRSOYAN, A.I.: Passive Statistical Methods for the Determination of Reactor Parameters. Statistical Methods in Experimental Reactor Kinetics and Related Techniques, Proc.Symp. Petten, Dec. 12-19, 1967. RCN-98.

[3.7] ROBINSON, J.C.: Analysis of Neutron Fluctuation Spectra in the Oak Ridge Research Reactor and the High Flux Isotope Reactor, ORNL-4149, Oak Ridge National Laboratory /1967/.

[3.8] STORRER, F.: Temperature Response to Power, Inlet Coolant Temperature and Flow Transients in Solid Fuel Reactors, APDA-132, Atomic Power Development Associates, Inc., /1959/.

[3.9] VÁRKONYI, L.: Reconstruction of the WWR-S Reactor in Budapest, /In Hungarian/ Atomtechnikai Tájékoztató 10, 633 /1967/

[3.10] MOGILNER, A.I., Private communication.

[3.11] KOSÁLY, G. and M.M.R. WILLIAMS, Atomkernenergie 18, 203 /1971/.

[3.12] WILLIAMS, M.M.R.: Reactivity Changes Due to the Random Vibration of Control Rods and Fuel Elements, Nucl. Sci. Eng. 39, 144 /1970/.

[3.13] ROBINSON, J.D.: An Introduction to Random Vibration, Edinbourgh Univ. Press 1963.

[3.14] STEPHENSON, S.E., D.P. ROUX, D.N. FRY: Neutron Fluctuation Spectra in the Oak Ridge Research Reactor, ORNL-TM-1401, Oak Ridge National Laboratory, 1966.

[3.15] FRY, D.N., J.C. ROBINSON: Neutron Density Fluctuation as a Reactor Diagnostic Tool. Paper for presentation at Conference on Incipient Failure Diagnosis for Assuring Safety and Availability of Nuclear Power Plants, Gatlenburg, Tennessee, Oct.30 - Nov.1, 1967.

[3.16] BENTLEY, P.G., D.G. DAWSON: Fluid Flow Measurement by Transit Time Analysis of Temperature Fluctuations, Trans. of the Soc. of Inst. Techn. /Sept. 1966/, 183 /1966/.

[3.17] TERMAAT, K.P.: Fluid Flow Measurements Inside the Reactor Vessel of the 50 MWe Dodewaard Nuclear Power Plant by Cross Correlation of Thermocouple Signals, Journal of Physics E.: Scientific Instruments 3, 589 /1970/.

[3.18] MIKA, C., K.H. RAES, D. STEGEMAN: Coolant Flow Measurements by Correlated Thermocouple-Signals. Paper presented at the IAEA Specialist Meeting on Analysis of Measurements to Diagnose Potential Failures 10-11 April 1972. Rome.

[3.19] KOSÁLY, G. and L. MESKÓ: Investigation of the Cross Correlation Function of Coolant Temperature Fluctuations via the Axial Dependent Two Point Model of Heat Transfer. Submitted for publication to Atomkernenergie.

4. EXPERIMENTAL POWER-REACTOR NOISE STUDIES

EDITED BY D. PALLAGI*

ABSTRACT

Power-reactor noise studies have been carried out in this Institute since the mid-sixties. The initial aim of the measurements was to establish the power-noise spectrum of the WWR-S reactor under normal operational conditions.

Later, investigations were centred mainly on the reliability of detecting bulk boiling by analysis of the noise deriving from core ionization chambers. The measuring arrangement and the results and conclusions drawn from these experiments are described here.

A recent problem to be tackled is the determination by cross-correlation method of the cooling water velocity in given channels of the reactor core. The present report describes the measuring arrangement and discusses the results obtained up to date.

4.1 Introduction

Exploration of the technological aspects of nuclear reactor noise was instigated in this Institute by the fundamental theoretical work of the director, L. Pál [4.1]. The first measurements in this field were performed in 1965, on the Institute's WWR-S reactor, in order to study the output power spectrum under normal operating conditions [4.2]. A main obstacle to this work, however, was soon found to be the cumbersomeness of the data-processing due to the lack of adequate computing facilities, which led to suspension of the measurements for a time. The experiments were resumed in 1968 when an ICT-1905 computer became available for on-line evaluation of the

*Acknowledgements

The editor is indebted to S. Horányi for his valuable participation in the measurements as well as to Messrs. F. Szlávik, G. Kozmann and P. Pellionisz for their aid in the needed special instrumentation.

power noise auto-correlation function and the noise spectra [4.3]. These measurements, too, the first to be made on-line at the Institute, had to be interrupted owing to the overload of the machine. Since 1970 the KORALL-B digital polarity correlator [4.4] has been available as the basic equipment for systematic and thorough study of reactor noises.

The ultimate aim of the noise studies is to develop a measuring method and equipment which would permit the forecasting of any operational failure of the reactor from information furnished by the noise. The reactor accidents reported up to now are sufficient demonstration that an entirely satisfactory solution to this problem is still to be found.

This report deals with two partial results of interest achieved within the scope of this long-term programme - bubble detection and fluid--flow measurement. Although a large amount of information has been collected already from measurements performed under different operational conditions of the reactor /noise pattern library/, no definite conclusions can be drawn yet from the available data.

4.2 Measurements

4.2.1 Detection of bulk boiling /bubbling/ [4.5]

The measurements to be described here concern the reliability of detecting water boiling /bubbling/ occuring at any point of the core by analysing the noise of the "out-of-core" ionization chamber current. The out-of-core detection of local boiling already proved to be a successful field of reactor diagnostics elsewhere [4.6].

The WWR-SM reactor

The WWR-SM reactor is a reconstructed version of the original WWR-S type reactor known from the literature [4.7]. Its main characteristics are:

- 5 MW nominal power
- beryllium-reflected core fuelled by WWR-M type fuel elements
- forced cooling by distilled water under pumping
- shielding by layers of water, iron and heavy concrete.

A notable feature is the positioning of the ionization chambers so that they are not submitted to the oscillating effects of flowing coolant water.

Bubble formation

Water boiling was simulated for the measurements by forcing air

into the core through a thin pipe situated in the irradiation channel. At the pipe end passing into the core was mounted a special head around which tiny bubbles could be formed under the effect of a low overpressure as if bulk boiling had started at this point of the core. A precision pressure reductor served for adjusting and maintaining the overpressure at a constant level.

Measuring arrangement and data processing

A block diagram of the measuring and data processing arrangement is shown in Fig. 4.1.

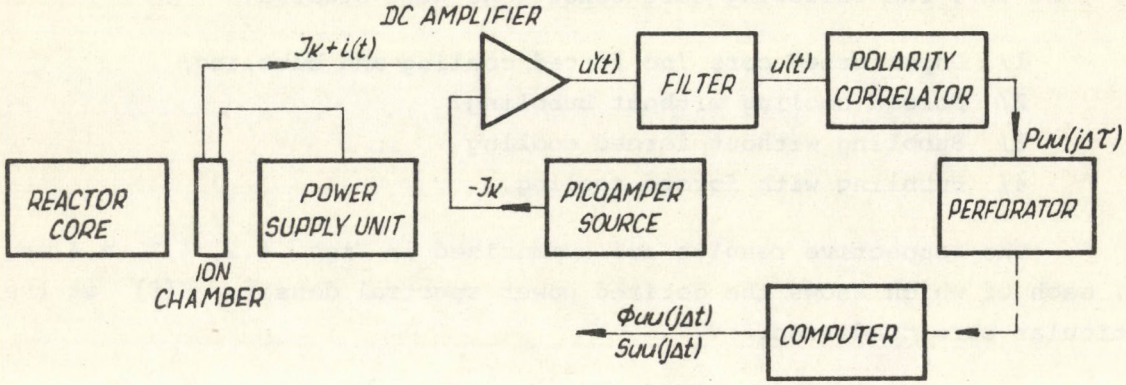

Fig. 4.1

Block diagram of the measuring arrangement and data-processing set-up for the detection of bulk boiling

The gamma-compensated ionization chamber used for detecting the thermal neutron flux is a KNK-53 model with a sensitivity of $2 \cdot 10^{-14}$ A/nvt. The flux-proportional signal is amplified by a d.c. amplifier /picoammeter/. A compensating current in proportion to the mean signal value is applied to the input of the amplifier by a Keithley Mod. 261 Picoampere Source, to exactly cancel the d.c. component of the output, so that only the fluctuation of the chamber current /i.e. the noise information/ is amplified to the required level. This amplified signal is sent on through a low-pass filter, adjusted to a cut-off frequency of 10 cps, to the digital polarity correlator formed by a NTA 512/B Amplitude Analyzer together with the special KORALL-B plug-in unit /see 1.1.2/. The chosen sampling frequency was 20 Hz, the maximum delay τ_{max} = 8 sec, and 15-20 minute runs were allowed for each measurement.

Assuming a Gaussian distribution of signals, there is an exact relationship between the measured polarity correlation and the true correlation function /see eq. /1.2//.

As the first step in further data-processing of the polarity correlogram, the true /normalized/ correlation function is evaluated on an ICT 1905 computer with the help of the RY-09 /FORTRAN/ program. This is then smoothed /filtered/ by applying the HANNING function, and finally Fourier transformed. The computer displays the data of the correlation function and the power density spectrum digitally and records both functions in a single coordinate system.

Results and conclusions

A reactor power of 20 kW was chosen for the measurements as this required no forced cooling and supplied a sufficently high ion-chamber current /~20 μA/. The following core conditions were studied:

1/ Unperturbed core /no forced cooling and bubbling/
2/ Forced cooling without bubbling
3/ Bubbling without forced cooling
4/ Bubbling with forced cooling.

The respective results are summarized in Figs. 4.2, 4.3, 4.4 and 4.5, each of which shows the derived power spectral density S(f) at the particular core condition.

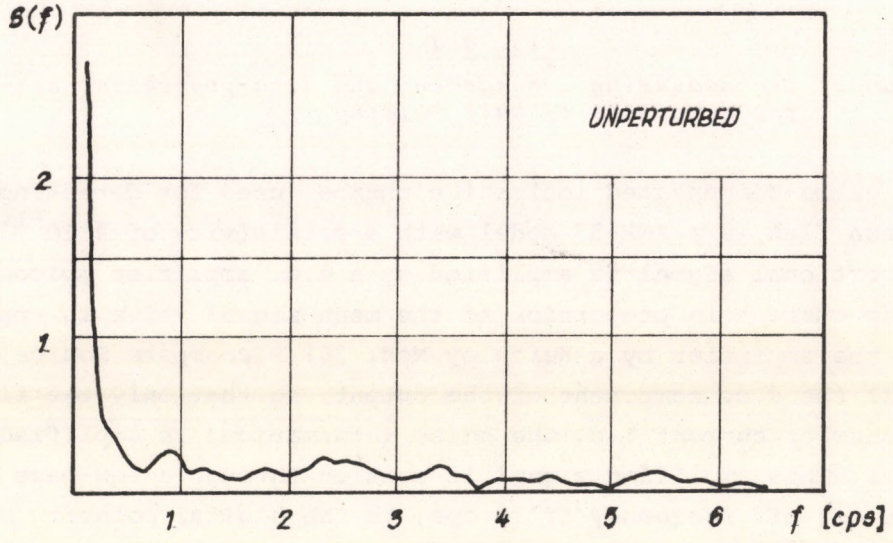

Fig. 4.2

Power spectral density function under unperturbed core conditions

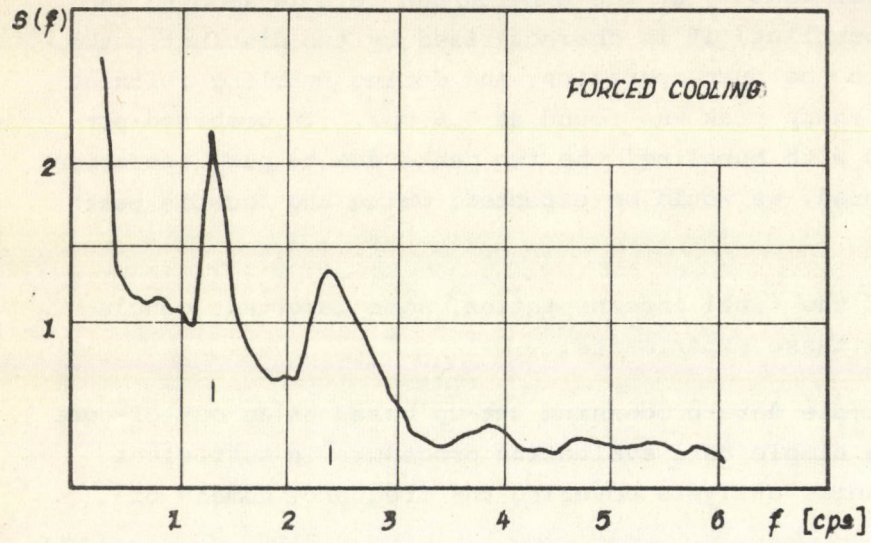

Fig. 4.3

Power spectral density function under conditions of forced cooling without bubbling

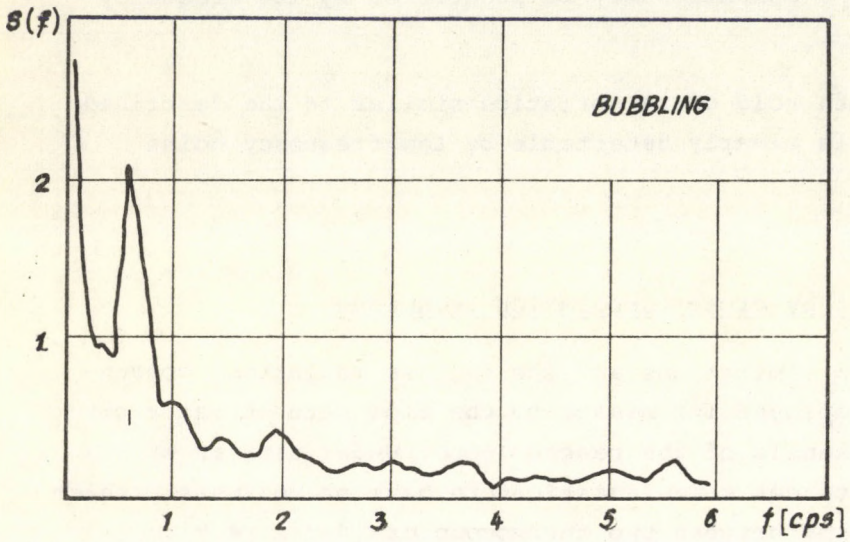

Fig. 4.4

Power spectral density function under conditions of bubbling without forced cooling

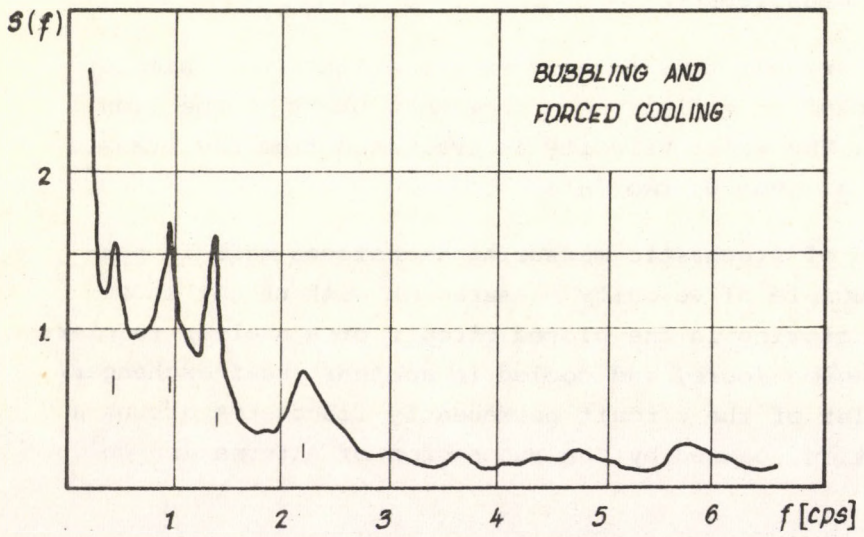

Fig. 4.5

Power spectral density function under conditions of bubbling with forced cooling

The power spectral density at the unperturbed core is smooth; in forced cooling /without bubbling/ it is characterized by two distinct peaks at 1.3 and 2.4 cps, due to the pump operation; and during bubbling /without forced cooling/ a rather sharp peak was found at 0.6 cps. In combined perturbation /forced cooling with bubbling/ the two peaks due to pump operation remain practically unaltered, as would be expected, while the "bubble peak" exhibits a "splitting".

Independently of the final interpretation, some important conclusions could be drawn from these experiments:

- This rather simple data-processing set-up based on an out-of-core detector and a simple data evaluating procedure is sufficient for reliable noise analysis covering the frequency domain of 0-10 cps.
- A particular core condition may be identified by low-frequency noise analysis.
- Bulk boiling with void characteristics similar to the described simulated case is clearly detectable by low-frequency noise analysis.

4.2.2 Velocity measurement by cross-correlation technique

Owing to geometric limitations and the intense radiation, conventional methods cannot be employed for measuring the flow rate of water circulating in the cooling channels of the reactor core. Under similar or comparably adverse circumstances some investigators have solved this problem by measuring the transit time between two thermocouples [4.8], [4.9].

Principle of the measurement

The principle of transit-time measurement is attractively simple. Two thermocouples are mounted at a distance $\underline{s}$ from each other in the flow path of the cooling water. The water velocity is evaluated from the transit time $\underline{t}_o$ over the distance $\underline{s}$ given by two data.

The fast progress of stochastic measuring techniques made it possible to utilize this principle of velocity measurement without any inconvenience. Since the water flowing in the closed circuit of a nuclear reactor is always heated in one region /core/ and cooled in another /heat exchanger/ its temperature at any point of the circuit permanently fluctuates around a given value. This fluctuation, caused by the succession of alternating colder

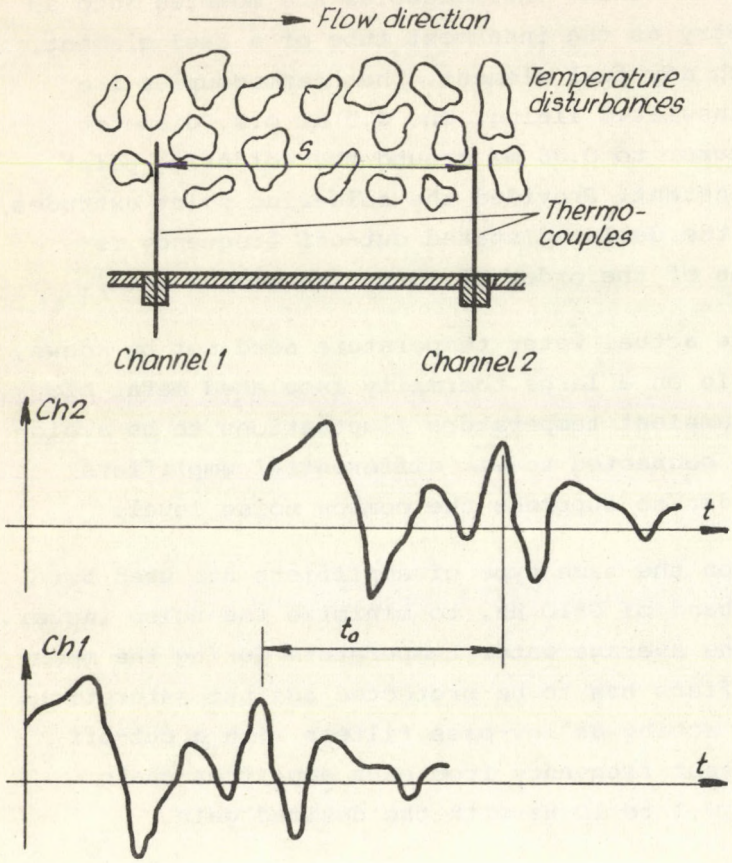

Fig. 4.6

Principle of coolant flow-rate measurement by cross-correlation technique

and warmer packets, is sensed by an appropriately chosen thermocouple the output voltage of which reflects the stochastic temperature fluctuations, as shown by the time curves in Fig. 4.6. If the distance s is chosen such that the flow pattern is not much distorted between thermocouples 1 and 2, the U_2 time curve will, except for a time lag t_o, have essentially the same shape as the U_1 time curve. The time lag, or transit time t_o can be readily determined from the cross-correlation function of the two time curves:

$$\phi_{12}(\tau) = \lim_{T\to\infty} \frac{1}{T} \int_0^T u_1(t)\, u_2(t+\tau)\, dt$$

This reaches a maximum with $\tau = t_o$ which can be read directly from the plot.

Measuring arrangement and data-processing

The block diagram of the measuring arrangement is given in Fig. 4.7.

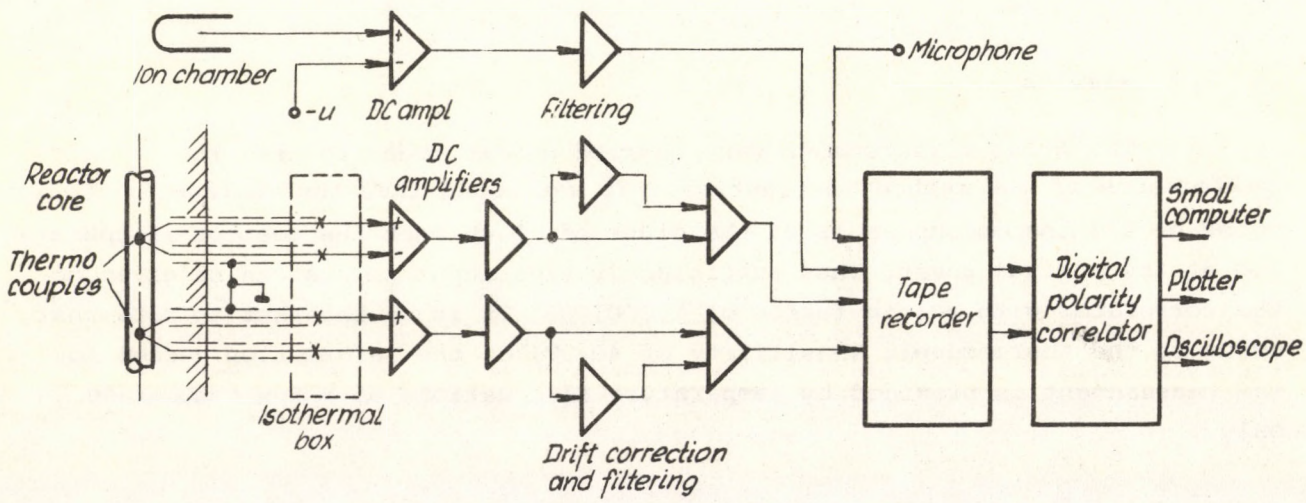

Fig. 4.7

Block diagram of the measuring arrangement and data-processing set-up for determination of coolant velocity

The two Sodern "Thermocoax" 2ABAc thermocouples are mounted into an aluminium tube of the same geometry as the innermost tube of a fuel element and can thus be interchanged with any fuel element. The thermocouples are canned in stainless steel with insulated lining. The 0.5 mm o.s. diameter has been reduced by the manufacturer to 0.35 mm around the soldering point in order to minimize the time constant. Provided the soldering point extrudes from the canning by about 5 mm, the declared/stated cut-off frequency is under our experimental conditions of the order of 10 Hz /catalogue data/.

Since in this method the actual water temperature need not be known, the cold points were chosen to lie on a large thermally insulated metal block, which permits interference from ambient temperature fluctuations to be avoided. The thermocouple outputs are connected to dc. differential amplifiers with a gain factor of 1000 in order to suppress the common noise level.

For further amplification the same type of amplifiers are used but transmitting only the frequency band of 0-10 Hz, to minimize the noise factor. Owing to the slow variation of the average water temperature during the measurement, set II of the main amplifiers has to be protected against saturation. This is achieved by amplifiers V acting as low-pass filters with a cut-off frequency of 0.1 Hz. Thus the output frequency from each amplifier chain generates only the spectrum from 0.1 to 10 Hz with the desired gain.

The basic unit of the measuring arrangement is the digital polarity correlator, which calculates the polarity correlation function, equivalent for our purpose to the true correlation function. The value of $\tau_{max} = k_{max}\Delta\tau$ is chosen such that the $\tau = t_o$ delay can be easily read. The correlator can calculate the function at points k_{max} = 64, 128, 256, and $\Delta\tau$ is variable in a wide range. The correlator output is displayed on oscilloscope and plotter. A perforator can be interfaced with the TPA small computer if Fourier transformation is needed.

Results

The first measurements were carried out in order to test the performance of the method in practice. It was found that the voltage noise of the thermocouples is of the order of 1 μV when the reactor is operating at its nominal power. Thus sufficiently high input pulses can be given to the correlator with a gain factor of 1,000,000. It is of interest to note that, owing to the thermocouple sensitivity of 40 μV/°C, the information needed for the measurement is provided by temperature fluctuations of a few centigrade only.

As examples, the cross-correlation functions generated at flow rates of $Q = 400\ m^3/h$ and $Q = 800\ m^3/h$ are presented in Fig. 4.8. The t_o time delay is readily estimated even visually, nevertheless the accuracy could be much improved by computer fitting. In Fig. 4.9 the values measured by conventional method /with a device in the primary circuit, off-core/ are compared with those of the correlation method. The agreement is convincingly good.

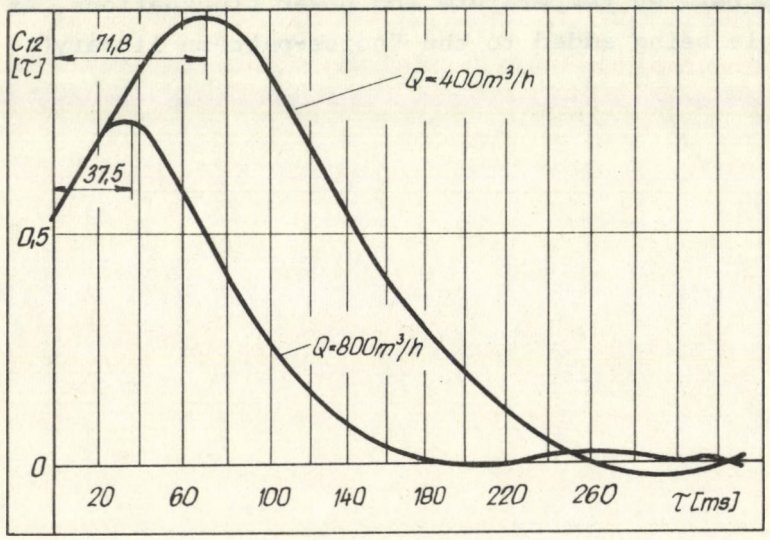

Fig. 4.8

Cross-correlation functions of thermocouple signals

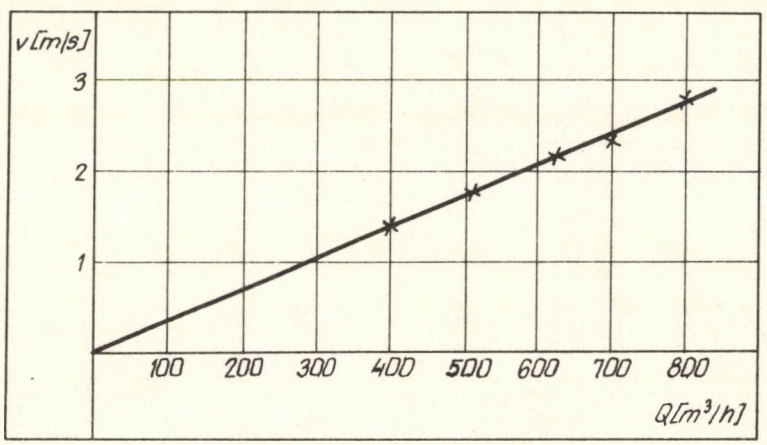

Fig. 4.9

Results of the velocity measurements

4.2.3 Present measurements

The Telefunken MAS 54 four-channel magnetic tape recorder supplied by the Agency offers the possibility of recording three analogue /+a reference/ signals. We are now analyzing the noise signals from two thermocouples and one ionization chamber in order to check the accuracy of the velocity measurements as well as to study the temperature fluctuation spectrum and the relationship between temperature and power fluctuations. At the same time new information is being added to the "noise-pattern library".

4.3 References

[4.1] PÁL, L., On the Theory of Stochastic Processes in Nuclear Reactors. Nuovo Cimento /Suppl./7. 1958. Series 10, 25-42

[4.2] PELLIONISZ, P., SZATMÁRY, Z., TURI, L., Noise Measurements on the WWR-S Reactor, 4th Conf. on Reactor Physics and Techn., Budapest, 1965

[4.3] SZATMÁRY, Z., VALKÓ, J., An On-line Spectral Analysis of Reactor Noise, Nukleonik, 12, 208-211 /1969/

[4.4] PELLIONISZ P., SZLÁVIK, F., Digitális készülékek korrelációs függvények felvételére. Mérés és Automatika, 15, 260-264 Budapest, /1967/

[4.5] PALLAGI, D., HORÁNYI, S., Power Reactor Noise Studies Using a Polarity Correlator. Report KFKI 71-31, 1971

[4.6] FRY, D.N., KRYTER, R.C., ROBINSON, J.C., Investigation of Boiling Detection in HFIR Using out-of-core Instrumentation. Nucl. Science Symp., New York, 1970

[4.7] GONCHAROV, V.V., Some New and Rebuilt Thermal Research Reactors. 2nd Conf. on the Peaceful Uses of Atomic Energy, Geneva, 1958 P/2185

[4.8] BENTLEY, P.G., DAWSON, B., Fluid Flow Measurement by Transit Time Analysis of Temperature Fluctuations. Trans. Soc. Instr. Technology, 183-192 /1966/

[4.9] TERMAAT, K.D., Fluid Flow Measurements Inside the Reactor Vessel of the 50 MWe Dodewaard Nuclear Power Plant by Cross-correlation of Thermocouple Signals. J. of Physics, E 3, 589-593 /1970/

5. CORRELATION METHODS IN NEUTRON SPECTROMETRY

EDITED BY P. PELLIONISZ*

ABSTRACT

A short summary is given of the new experimental methods developed and used in correlation neutron spectroscopy studies at the Institute.

The first application of the statistical chopping technique had been before the I.A.E.A. Research Contract 855/R1/RB; the research activity has been widened during the period covered by the contract. Some of the results have been achieved in cooperation with other scientific institutes /Joint Institute for Nuclear Research, Dubna; Institut Laue-Langevin, Grenoble/.

Equipment for spin-flipping and magnetic pulsing as well as a mechanical correlation chopper have been built. New methods have been developed and applied for correlation time-of-flight spectrometry and diffractometry and for filtering out certain spectrum components or separating elastically from inelastically scattered neutrons. The application of correlation methods has been extended to pulsed neutron sources.

5.1 Correlation-type spectrometry

5.1.1 Time-of-flight spectrometer with magnetical pulsing

The correlation-type technique of time-of-flight spectroscopy was first introduced in neutron scattering research about five years ago, e.g. [51] [52]. Its principle is very simple: the pulse-response function $S(\tau)$ of a linear system /i.e. its conventional time-of-flight distribution function/ is proportional to the cross-correlation function

* Acknowledgement

The editor is indebted to Prof. L. Pál /C.R.I.P., Budapest, Hungary/ and to Prof. H. Maier-Leibnitz /I.L.L., Grenoble, France/ for many clarifying discussions. Several new methods were elaborated and measurements performed in cooperation with different researchers: the contributions of Messrs. N. Kroó, F. Mezei, F. Szlávik and J. Vizi in particular are highly appreciated.

$$S(\tau) = \phi_{MZ}(\tau) = \lim_{T\to\infty} \frac{1}{T} \int_0^T M(t-\tau)Z(t)dt. \qquad /5.1/$$

Here $M(t)$ is an input signal of random character /i.e. having an auto-correlation function of the δ -type/ and $Z(t)$ is the response on the system's output:

$$Z(t) = \int_0^t M(t-\tau)S(\tau)d\tau. \qquad /5.2/$$

In a neutron scattering experiment of correlation type the monoenergetic neutron beam incident on the sample is randomly modulated and the neutrons are counted at a given scattering angle by a detector placed at a given distance from the sample. When the cross-correlogram between the modulation and detected events is calculated one gets the time-of-flight density function characteristic for the sample investigated.

In the first experiments the pseudo-random modulation was achieved by means of a controlled neutron spin flipper and data-processing was performed by the KORALL-A digital correlator developed specially for this application /see 1.1.1/. Pulses from the neutron detector were stored during the measurement, and at the end the device automatically performed the correlation computation.

The main advantage of the correlation method stems from the fact that non-correlated background is strongly reduced in the result. The relative statistical accuracy of the spectrum is variable, depending on the duty-cycle of the on-off sequence used in the pseudo-random modulation and on the shape of the spectrum itself. Mathematical details and error analysis have been thoroughly discussed by several authors [5.3], [5.4], [5.5].

5.1.2 Time-of-flight spectrometer with Fermi chopper

The spin-flip chopping technique introduced by our Laboratory has proven to be an original and successful method, but it has certain limitations of application. Its neutron economy is generally not very good; higher flux values can be achieved when chopping is done by a mechanical device /e.g. a rotating disk with one or more "windows" for neutrons/.

The construction of a rotating statistical chopper raises a host of problems, primarily in respect of the mechanics. To illustrate these difficulties, the main specifications of the rotating device constructed for correlation spectrometry in our Laboratory are:

- diameter: 680 mm
- speed of rotation: 6000 rpm
- dimension of an elementary neutron window: 8 x 40 mm
- number of neutron windows: 255
- sequence of neutron windows: maximum length binary pseudo-random sequence /n = 8/

In order to obtain the necessary dynamic balance of the disk, window-segments are of Al, while neutron-absorbent segments are special combinations of araldite and absorbent Gd_2O_3.

The schematic set-up of the correlation time-of-flight spectrometer put in operation in 1970-71 is shown in Fig. 5.1. It is suitable for the investigation of both powder and monocrystalline samples. The detector set-up permits simultaneous measurements at four angles. As the driving mechanism of the chopper is not stabilized, data collection is controlled by an automatic unit which inhibits the input signals to the memory whenever the difference between the actual and the nominal values of the chopper's period exceeds a given error limit. The cross-correlation function is calculated off-line by one of the TPA 1001 small computers developed and manufactured in the Institute. The program can carry out calculations for up to 1020 channels, averaging, smoothing with a pre-measured experimental resolution function, appropriate shifting or selection of a spectrum section, printing, plotting, etc.

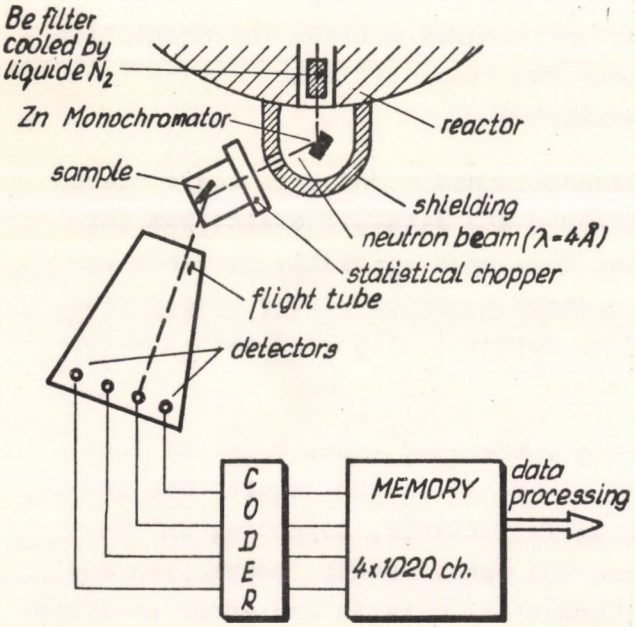

Fig. 5.1

Schematic set-up of the correlation time-of-flight spectrometer

The correlation method results in a substantial improvement of the resolution of diffraction measurements, as can be seen from a comparison of the diffractograms reproduced in Fig. 5.2 and Fig. 5.3.

At present the equipment is being employed to study liquid crystal, by inelastic neutron scattering. In Fig. 5.4 a comparison is shown between solid phase and liquid-crystal phase, of para-asoxy-anisol while in Fig. 5.5 the solid phase is compared with the isotropic liquid phase. Both spectrum parts were taken in the region of the elastic line.

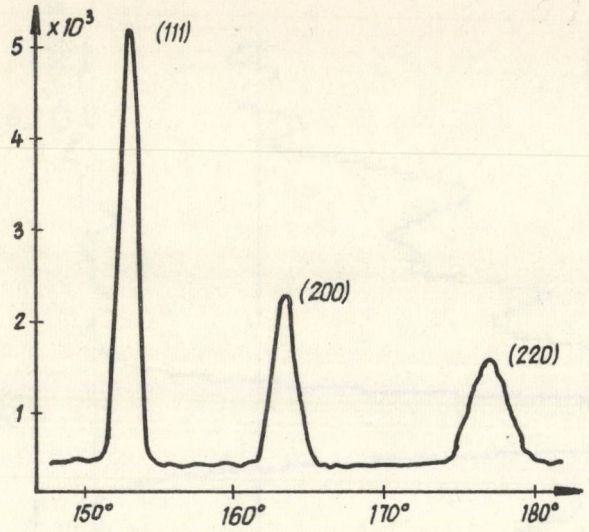

Fig. 5.2

Diffractogram of a Ni-powder sample, as measured by a conventional diffractometer

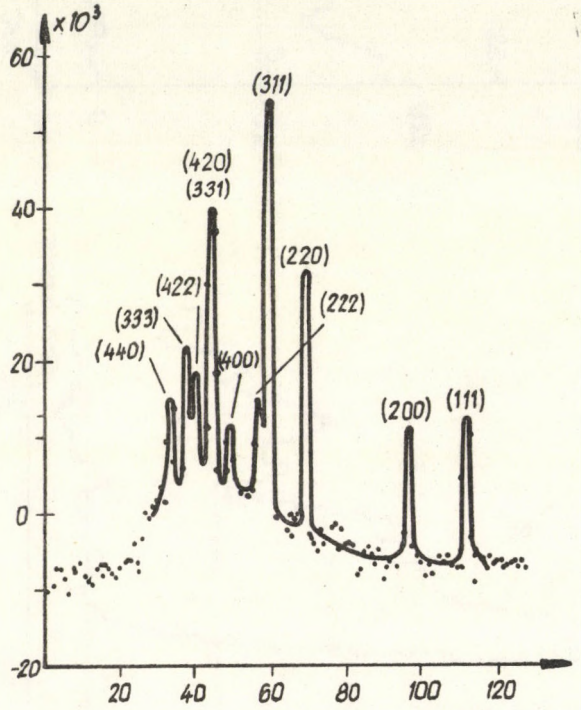

Fig. 5.3

Diffractogram of a Ni-powder sample, as measured by the correlation equipment

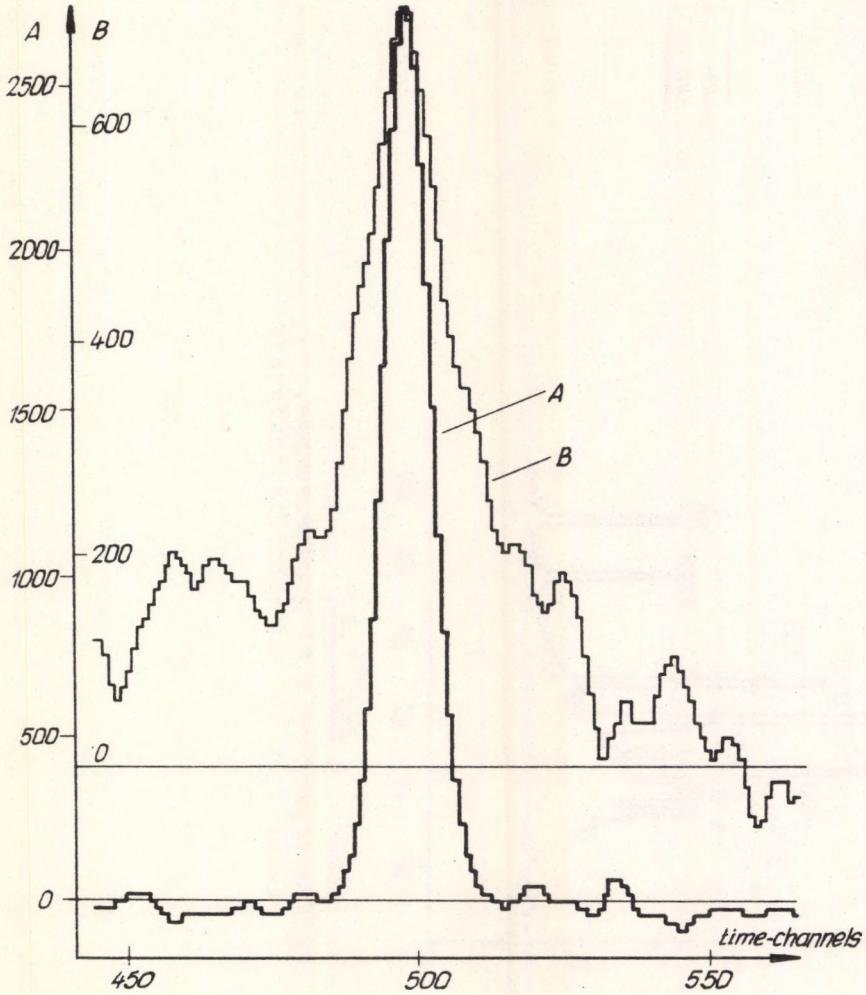

Fig. 5.4

Time-of-flight spectrum of para-asoxyanisol in solid (A) and liquid-crystal (B) phase

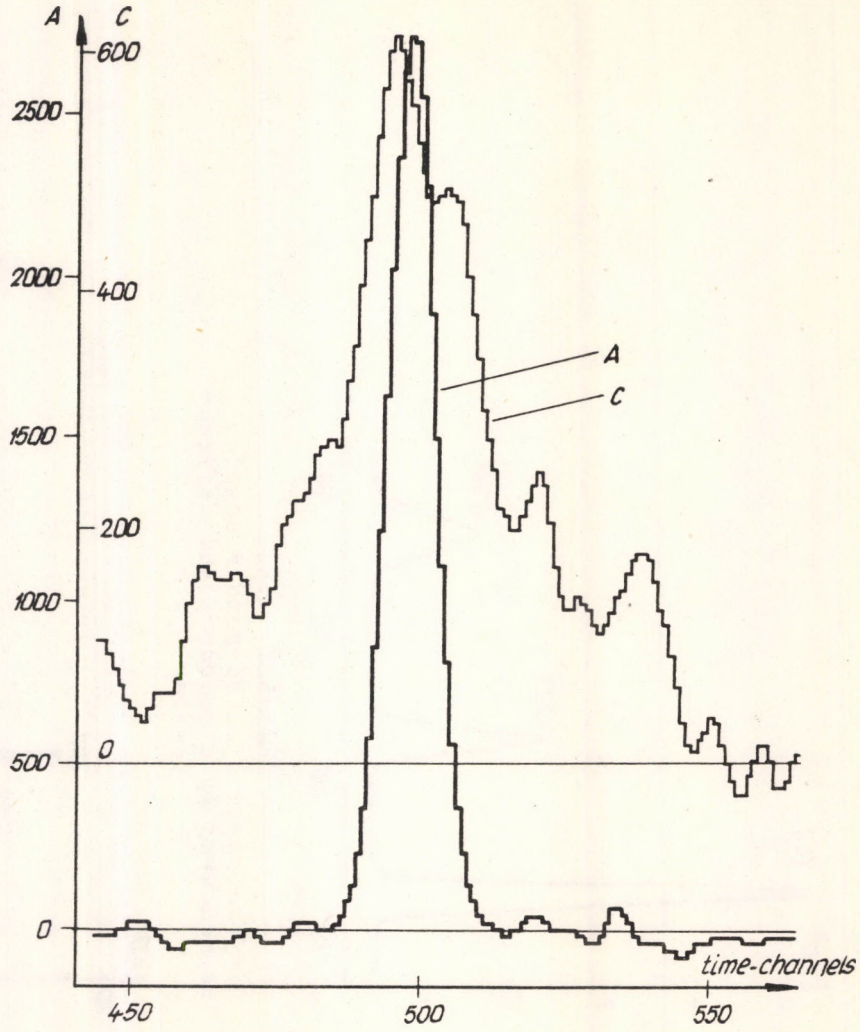

Fig. 5.5

Time-of-flight spectrum of para-asoxyanisol in solid (A) and isotropic liquid (C) phase

5.2 Pseudo-random modulation methods in polarized neutron diffractometry

5.2.1 Time-of-flight analysis of polarization effects

In polarized neutron diffraction research the problem of separating and determining higher-order reflections and inelastic magnetic scattering contributions is sometimes of considerable importance. In the course of studies in the field of correlation methods we have developed several techniques as alternatives to the usual practice in polarized neutron diffractometry [5.6],[5.7].

With polarized neutrons it is necessary to compare counting rates for the two opposite neutron polarization directions. Generally, this is achieved by taking counts while a neutron spin flipper device is slowly turned on and off alternately. However, not all the detected neutrons are monoenergetic, and higher-order and inelastically scattered contributions can falsify the comparison of the measured counting rates.

In order to overcome these difficulties we have replaced the alternating on-off modulation by a modulation of pseudo-random type. In this way the needed on-off time ratio is retained and, with the aid of the correlation time-of-flight method, no more than two counting rate values but two time-of-flight spectra have to be compared. A schematic set-up of the experiment is shown in Fig. 5.6. The monoenergetic neutron beam is modulated in the direction of polarization by a controlled spin flipper. The modulation is a periodic function of time

$$X(t) = \sum_i x_i \, \psi(t - t_i) \qquad /5.3/$$

where x_i is a pseudo-random binary sequence taking values of +1 and -1, while $\psi(t)$ is the pulse-shape function of the elementary modulation in time.

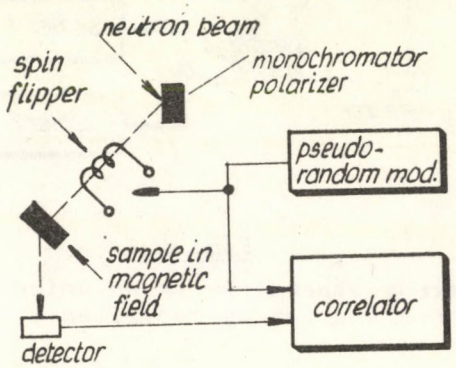

Fig. 5.6
Schematic set-up of a polarized neutron time-of-flight spectrometer

A difference spectrum $[S_\uparrow(\tau) - S_\downarrow(\tau)]$ is obtained by computing the cross-correlogram between the detected counting rate $Z(t)$ and the modulator sequence $x(t)$:

$$\Phi_{xZ}(\tau) = \frac{1}{T}\int_0^T Z(t)\, x\, (t-\tau)dt = \frac{1}{2}\int_0^\tau \Phi(\tau-t)\left[S_\uparrow(t)-S_\downarrow(t)\right]dt+\text{const} \qquad /5.4/$$

It can be seen that $\phi_{xz}(\tau)$ describes the resolution-broadened time-of--flight spectrum of the modulated magnetic scattering effects, while the non-magnetic scattering is contained in a uniform background.

A series of successful measurements with the aid of this method has been performed. The overall polarization efficiency of the Co /8% Fe/ monochromator for the [220] reflection is found to be about 15%. A pseudo--random sequence of 255 steps and 50% duty-cycle is applied.

5.2.2 Energy separation from polarization effects

In many cases, when only the difference of spectra corresponding to a given energy is of interest, the disturbing effects may be simply filtered out [5.6], [5.7]. The same diffractometer arrangement as in the previous method can be applied except that two scalers are used instead of the correlator /Fig. 5.7/. The modulator signal is delayed by a time-distance corresponding to the time-of-flight of the neutrons under observation, and the counts are taken by the two scalers alternately, on signals from the delayed modulator. Neutrons of the given energy scattered with spin-plus are counted in Scaler 1, those with spin-minus in Scaler 2. As the unwanted contribution is statistically distributed between the scalers, the difference of the counts gives directly the value of the modulated magnetic scattering.

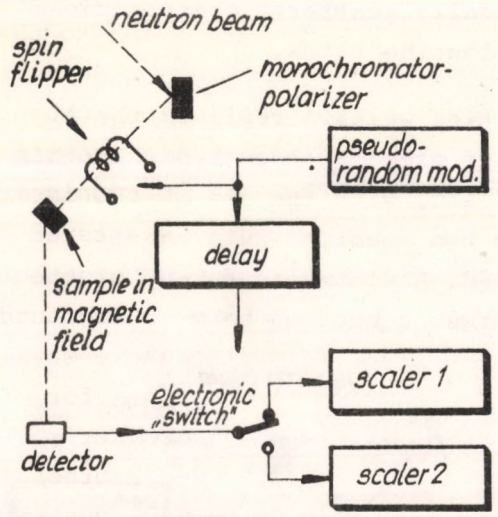

Fig. 5.7

***Energy** separation in polarized magnetic scattering experiments*

5.3 Statistical separation and filtering methods

5.3.1 Separation of elastically and inelastically scattered neutrons

In the time-of-flight method for neutron diffraction investigations a polyenergetic neutron beam is scattered on the sample and the intensity vs time-of-flight spectrum is measured at a fixed angle. The elastic scattering effect that is to be measured, however, is more or less contaminated by inelastic scattering components. In order to eliminate the inelastic contribution, a new method was designed [5.8] which permits the separate registration

of inelastically and elastically + inelastically scattered neutrons. The schematic set-up and time-diagram of such an experiment is shown in Fig. 5.8.

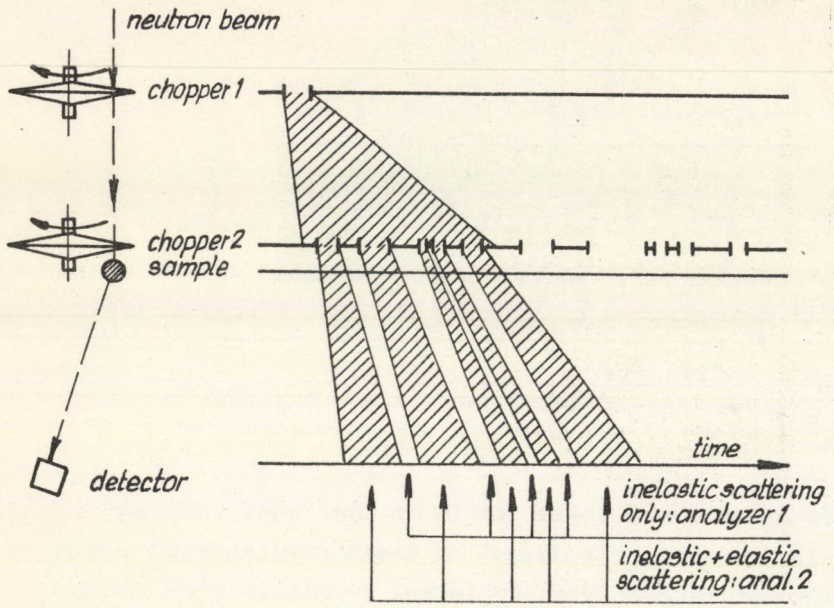

Fig. 5.8

Schematic set-up and time diagram of a conventional time-of-flight measurement with separation of inelastic/elastic scattering

The Chopper 1 - Sample - Detector assembly works as a conventional time-of-flight spectrometer, while Chopper 2, placed close before the sample, performs an additional chopping of pseudo-random character. At the detector there are two kinds of detection possibilities, according to the "projected" pattern of the statistical chopper: namely, there are time intervals when only inelastically scattered neutrons can be detected /apart from background/ and other intervals with no restriction. By measuring in two separate ways /i.e. by constructing two time-of-flight spectra and completing them for every time-of-flight value by continuously shifting the second chopper's program/ a complete time-of-flight spectrum for the inelastic and another for the elastic + inelastic scattering can be evaluated. The difference quantity between the two spectra is directly related to the desired elastic spectrum.

The generalized theory of this method is discussed in [5.8]. The influence of the duty cycle /open time fraction/ of the pseudo-random chopper, pulse shapes of the choppers, etc. are treated there in detail and the relative statistical error of the measurement is calculated as a function of the duty cycle for different spectrum and background parameters. The optimum value of the duty cycle is found to be nearly 0.5 in all practical case, provided no extreme conditions are present.

A second experimental solution was also devised for this separation problem [5.9] which combines the usual statistical chopper time-of-flight method [5.1] and the separation process described above. Here, both choppers are of a statistical character: a separation process is started at each slit of the first chopper and they are linearly superimposed /see Fig. 5.9/.

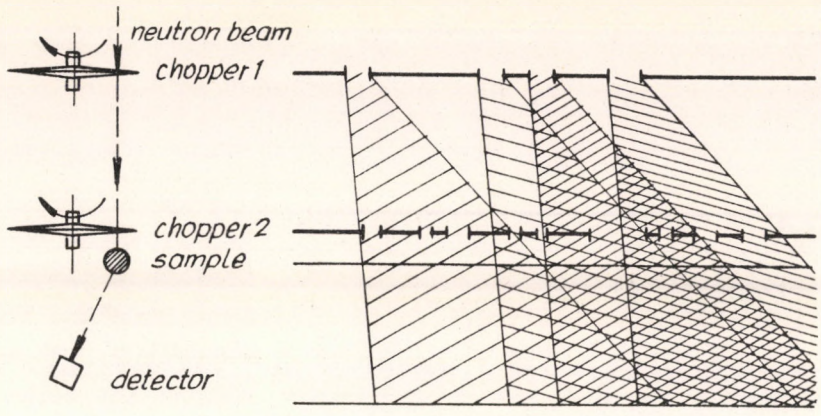

Fig. 5.9

Double statistical chopper for simultaneous time-of-flight measurement and separation of inelastic/elastic scattering

The elastic / not elastic decisions are taken while in the same time successive points of the correlogram are calculated at every registrated event /i.e. while sorting the detected neutron for different possible time origins at the first chopper/. When a certain origin and hence a certain time-of--flight value is taken, the time when the actual value of the second chopper must be inspected can be calculated on the basis of the given geometrical relations. /The actual value may be read e.g. from a memory containing the second chopper's program./ According to this information the event will be stored in one of the two separate multichannel memories, so that by systematic shifting of the second chopper's program two complete spectra can be evaluated.

The introduction of the correlation method at the separation arrangement increases its neutron economy, i.e. in most cases leads to a gain in statistical accuracy /or measuring time/ compared to the previous method. The gain, however, is always determined by the actual structure of the spectrum, just as in the conventional simple correlation method.

5.3.2 Statistical chopper for spectrum filtering

In neutron scattering experiments based on the correlation time-of--flight method the statistical accuracy of any given spectrum component is influenced by the character of all the other parts of the spectrum. When small peaks are to be measured and if high peaks could be filtered out, a considerable improvement in statistical accuracy could be obtained.

A method has been devised and tested [5.10] which achieves such a filtering by introducing a further pseudo-statistical modulation of the in-

cident beam and a corresponding on-off control of the detected intensity. Fig. 5.10 shows the schematic time-diagram of such an experiment.

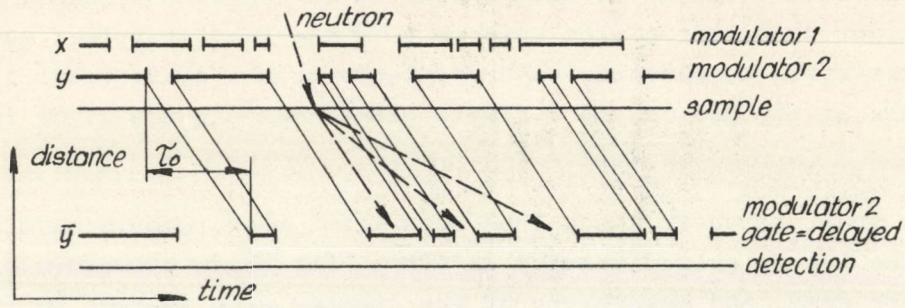

Fig. 5.10

Spectrum filtering by introducing modulator 2 and corresponding gating

Here the two modulations must be independent: x_i serves as a normal correlation reference, while y_{i+k} is the filtering reference. The pulses delivered by the detector are gated with a delayed square - wave version of the filtering sequence

$$\bar{y}_{i+k} = 1 - y_{i+k-\tau_o} , \qquad /5.5/$$

where τ_o is the time-of-flight value to be filtered. In other words, pulses are not taken into the correlation computation when they can have a prohibited energy. With other pulses a normal correlation computation is performed.

The generalized theory of the method, its statistical efficiency, the problems encountered in effectuating it, etc. are discussed in detail in ref. [5.10]. Experimental trials have been carried out using a chopper of the spin-flipper type, driven by two superimposed pseudo-random sequences, for simultaneous correlation and filtering with a modified KORALL-A correlator.

5.4 Correlation time-of-flight spectrometry at pulsed reactors

Recently, a new method was found for the application of correlation technique at pulsed neutron sources [5.11]. It was shown that if a white ingoing neutron beam is used, the entire two-dimensional scattering spectrum can be evaluated by correlation-type data-processing. A statistical chopper is operated far from the pulsed neutron source so that the neutron beam should be spread in time at the chopper site. The chopper is not synchronized to the reactor and its transmission function is not sensitive to the neutron

energy. The sample is located immediately behind the chopper. Scattered neutrons are detected after a flight path comparable with the reactor-chopper distance. The data obtained is then subjected to two-dimensional analysis /time-of-flight calculation with reference to the reactor pulse, and simultaneous correlation computation with reference to the statistical chopper/. The principle of the method and a simple error analysis are given in ref. [5.11].

In order to check the method some trial measurements have been performed at the IBR-30 pulsed reactor in Dubna. For these experiments 63 x 63 channels were used, and asynchrony of the chopper with respect to the reactor was controlled throughout. The results of a test run measured on a plexiglass scatterer are illustrated in Fig. 5.11., which shows the relations between incoming and outgoing energy of the scattered neutrons.

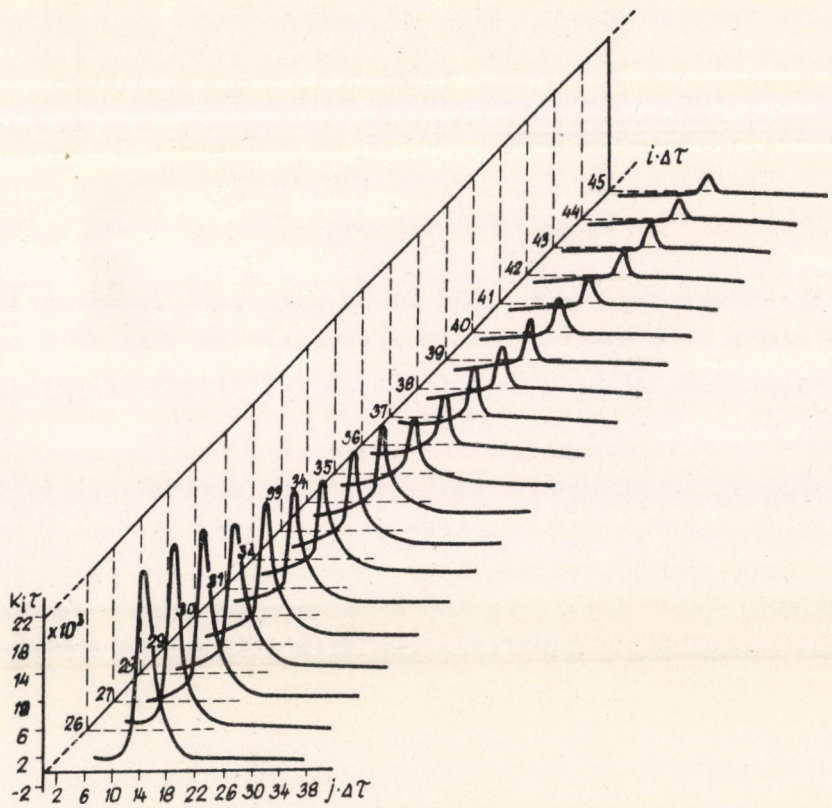

Fig. 11

Two-dimensional scattering pattern measured with the pulsed correlation method

5.5 References

[5.1] PÁL, L., KROÓ, N., PELLIONISZ, P., SZLÁVIK, F., VIZI, I., Neutron Inelastic Scattering Symp., Copenhagen, 1968. Vol. 2. 407

[5.2] GOMPF, F., REICHARDT, W., GLÄSER, W., BECKURTS, K.H., Neutron Inelastic Scattering Symp., Copenhagen, 1968. Vol. 2, 417

[5.3] JAN, R. von, SCHERM, R., Nuclear Instruments and Methods, 80, /1970/ 69

[5.4] HOSSFELD, F., AMADORI, R., Kernforschungsanlage Jülich, KFA Report Jül-684-FF /1970/

[5.5] HOSSFELD, F. AMADORI, R., SCHERM, R., Proceedings of the Panel Conf. on Instr. for Neutron Inelastic Scattering Research, VIENNA, 1969

[5.6] MEZEI, F., PELLIONISZ, P., Nuclear Instruments and Methods, 99, /1972/, 613

[5.7] MEZEI, F., PELLIONISZ, P., Neutron Inelastic Scattering Symp., Grenoble 1972. IAEA/SM-155/F-9

[5.8] PELLIONISZ, P., Nuclear Instruments and Methods, 92, /1971/ 125

[5.9] PELLIONISZ, P., Atomkernenergie, 17, /1971/ 277

[5.10] PELLIONISZ, P., KROÓ, N., Neutron Inelastic Scattering Symp., Grenoble 1972. IAEA/SM-155/F-8

[5.11] KROÓ, N., PELLIONISZ, P., Neutron Inelastic Scattering Symp., Grenoble 1972. IAEA/SM-155/F-6

ACKNOWLEDGEMENT

Though individual editors have been selected to write the different sections, it ought to be emphasized that the results are in most cases the products of close team-work. The authors are indebted to Prof. L. Pál and the following contributors:

Z. Gyimesi
S. Horányi
N. Kroó
L. Meskó
F. Mezei
J. Valkó
I. Vizi

62.014

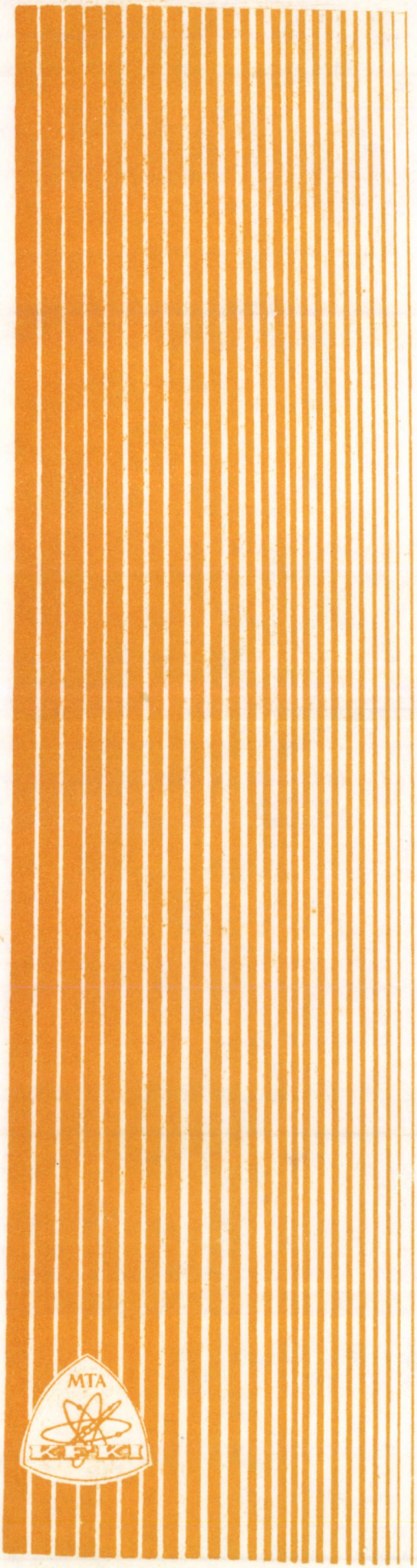

Kiadja a Központi Fizikai Kutató Intézet
Felelős kiadó: Szlávik Ferenc, a KFKI Műszer- és Méréstechnikai Tudományos Tanácsának elnöke
Szakmai lektor: Meskó László, Kosály György, Péter Attila, Kroó Norbert
Nyelvi lektor: T. Wilkinson
Példányszám 315 /utánnyomás/ Törzsszám: 73-8490
Készült a KFKI sokszorosító üzemében,
Budapest, 1973. május hó